EC Journals.ASM.org

Comparison of Switching and Biofilm Formation between *MTL*-Homozygous Strains of *Candida albicans* and *Candida dubliniensis*

Claude Pujol, Karla J. Daniels, David R. Soll

The Developmental Studies Hybridoma Bank, Department of Biological Sciences, The University of Iowa, Iowa City, Iowa, USA

***Candida albicans* and *Candida dubliniensis* are highly related species that share the same main developmental programs. In *C. albicans*, it has been demonstrated that the biofilms formed by strains heterozygous and homozygous at the mating type locus (*MTL*) differ functionally, but studies rarely identify the *MTL* configuration. This becomes a particular problem in studies of *C. dubliniensis*, given that one-third of natural strains are *MTL* homozygous. For that reason, we have analyzed *MTL*-homozygous strains of *C. dubliniensis* for their capacity to switch from white to opaque, the stability of the opaque phenotype, CO_2 induction of switching, pheromone induction of adhesion, the effects of minority opaque cells on biofilm thickness and dry weight, and biofilm architecture in comparison with *C. albicans*. Our results reveal that *C. dubliniensis* strains switch to opaque at lower average frequencies, exhibit a far lower level of opaque phase stability, are not stimulated to switch by high CO_2, exhibit more variability in biofilm architecture, and most notably, form mature biofilms composed predominately of pseudohyphae rather than true hyphae. Therefore, while several traits of *MTL*-homozygous strains of *C. dubliniensis* appear to be degenerating or have been lost, others, most notably several related to biofilm formation, have been conserved. Within this context, the possibility is considered that *C. dubliniensis* is transitioning from a hypha-dominated to a pseudohypha-dominated biofilm and that aspects of *C. dubliniensis* colonization may provide insights into the selective pressures that are involved.**

In the evolution of species, developmental programs rapidly evolve in response to the selective pressures of environmental change and decay when those selective pressures weaken or disappear (1–3). Decay is most obvious among strains within species with predominately clonal population structures (i.e., species that rarely undergo recombination), since they result in increased strain variability (4–7). A remarkable example of the apparent decay of developmental programs can be found in *Candida dubliniensis*, a close relative of the more common opportunistic yeast pathogen *Candida albicans* (8–11). *Candida dubliniensis* and *Candida albicans* diverged approximately 20 million years ago (12), soon after the Eocene/Oligocene period, at approximately the same time primates evolved. The two species share approximately 96% of their genes (13) and undergo similar developmental programs, such as filamentation (14, 15), white-opaque switching (16), and mating (16). However, while these developmental programs appear to have been highly conserved among strains of *C. albicans*, they are highly variable or diminished among strains of *Candida dubliniensis*. The two species also exhibit differences in a number of other traits, including the utilization of carbon sources (17–19), adherence to buccal epithelium in glucose-based medium (20), the induction of chlamydospores (21), the adhesive characteristics of mating cells in suspension (16), and the filamentous phenotype of cells in biofilms (22), although the last two differences were not reported for a variety of strains.

It has been suggested that degeneration of developmental programs, reflected in the variability between strains of *C. dubliniensis*, is due to differences in species-specific genes (13), differences in the expansion of select gene families (13), and pseudogenization (23). In addition, the high rate of genomic reorganization, reflected by highly variable and unstable karyotypes (24–26), has also been suggested as a cause. But there is one additional factor that, surprisingly, is rarely considered in studies of *C. dubliniensis* or even in reviews of *C. dubliniensis* variability and virulence, namely, the configuration of the mating type locus. The reason this omission is surprising is that in 2004 (16), an analysis of the mating type locus revealed that one-third of natural *C. dubliniensis* strains were *MTL* homozygous (**a/a** or α/α), compared to approximately 8% (27) for *C. albicans*. It has been demonstrated in *C. albicans* that *MTL*-heterozygous and *MTL*-homozygous cells differ dramatically both phenotypically and in their developmental potential. They differ in their capacity to switch between white and opaque (28, 29), their capacity to mate (29, 30), the functional traits of the alternative biofilms that they form (31–33), the signal transduction pathways regulating the formation of these alternative biofilms (32), the transcription factors targeted in alternative biofilm formation (32, 34), pheromone-induced adhesivity and gene transcription (32, 34–37), susceptibility to fluconazole, itraconazole, voriconazole, and flucytosine (27), and virulence (38). Because of the high level of *MTL* homozygosity among natural strains of *C. dubliniensis*, any unique phenotypic traits of *MTL*-homozygous strains must be discriminated to assess past studies of strain variability and the need for discrimination between *MTL* configurations in future studies.

To this end, we have initiated a comparison of the variability of *MTL*-homozygous *C. dubliniensis* strains with that of *MTL*-homozygous *C. albicans* strains for a number of characteristics re-

Received 31 August 2015 **Accepted** 23 September 2015

Accepted manuscript posted online 2 October 2015

Citation Pujol C, Daniels KJ, Soll DR. 2015. Comparison of switching and biofilm formation between *MTL*-homozygous strains of *Candida albicans* and *Candida dubliniensis*. Eukaryot Cell 14:1186–1202. doi:10.1128/EC.00146-15.

Address correspondence to David R. Soll, david-soll@uiowa.edu.

C.P. and K.J.D. contributed equally to this article.

Supplemental material for this article may be found at http://dx.doi.org/10.1128/EC.00146-15.

lated to white-opaque switching. The comparison includes the frequency of switching, maintenance of the opaque phenotype, the effect of CO_2 on switching, and the effects of pheromone on adhesion and the architecture of the biofilms formed. Our results demonstrate that *C. dubliniensis* strains exhibit lower mean frequencies of white-to-opaque switching, higher instability of the opaque phenotype, uniform absence of CO_2-induced white to opaque switching, more variability in the formation of the basal yeast cell polylayer of biofilms, a near-uniform conversion from an upper region of vertical hyphae to a mesh composed predominately of pseudohyphae, and a reduction in extracellular matrix (ECM). In marked contrast, white cells of *MTL*-homozygous strains of *C. dubliniensis* have retained uniform shape and size and uniform responsiveness to pheromone, as is the case in *C. albicans*. More surprisingly, even though *MTL*-homozygous biofilms of *C. dubliniensis* are on average significantly thinner than those of *C. albicans*, the average dry weight and the stimulation of dry weight by minority opaque cells are similar among strains of the two species. The reduction in switching frequency, the instability of the opaque phase, the variability of the opaque cell phenotype, the absence or loss of CO_2 induction, and the variability in biofilm architecture could all reflect the highly unstable genome of *C. dubliniensis*. However, the conservation or uniformity of other traits, including the uniform yeast phase phenotype of white cells, similar extant and variability of pheromone-induced adhesion, similar average biofilm dry weight, and similar minority opaque cell induction of biofilm dry weight, as well as the near-uniform transition from a predominately hyphal to pseudohyphal biofilm, together suggest that not all phenotypic traits are decaying and some differences may have evolved due to selective pressures different from those governing the phenotypic repertoire of *C. albicans*.

MATERIALS AND METHODS

Yeast strains and growth conditions. The *C. albicans* and *C. dubliniensis* strains used in this study and their *MTL* genotypes are listed in Tables S1 and S2 in the supplemental material. Cells were grown from frozen stocks and maintained at 25°C on agar plates containing supplemented Lee's medium (39, 40) containing 5 μg/ml phloxine B, which differentially stained opaque colonies and sectors red (41). Cells in the white or opaque phase were also verified microscopically prior to use. Cells used for each experiment were grown to stationary phase in liquid supplemented Lee's medium at 25°C for 48 h. The species status of strains was verified by PCR using the protocols of McCullough et al. (42) and Romeo and Criseo (43). Both methods use specific size polymorphisms to distinguish *C. albicans* from *C. dubliniensis*. While the method developed by McCullough et al. (42) separates the two species based on size polymorphism of the intron of the 25S rRNA gene, the Romeo and Criseo (43) approach identifies the two species based on *HWP1* polymorphisms. The two methods resulted in the same species identification for the strains tested.

Biofilm development. Biofilms were developed on silicone elastomers in the wells of cluster dishes in RPMI 1640 medium containing 165 mM MOPS (morpholinepropanesulfonic acid; pH 7.0) (referred to here as "RPMI medium"). Silicone elastomer discs were cut from 0.04-in.-thick silicone elastomer sheets (Bentec Medical), using a 10-mm biopsy punch (Acu-Punch; Acuderm, Inc.). The discs were washed and sterilized as previously described (35), placed in a 24-well cluster dish (Costar; Corning, Inc.), and incubated overnight in 2 ml of RPMI medium at 29°C. The temperature of 29°C was selected, since temperatures above 34°C induce opaque-to-white switching. The incubation medium in which the silicone elastomer discs were incubated was replaced with 2 ml of fresh RPMI medium containing 2×10^7 stationary-phase cells. Opaque cell stimulation of *MTL*-homozygous white cell biofilms was performed by adding a minority (10%) opaque cell mixture (1:1 ratio of *C. albicans* opaque P37005 **a/a** cells and opaque WO-1 α/α cells, or a 1:1 ratio of *C. dubliniensis* d81217 **a/a** cell and opaque d126423 α/α cells) to a majority (90%) of white **a/a** cells (36). The cells were allowed to adhere without agitation for 90 min at 29°C. After adhesion, the discs were removed and gently rinsed with Dulbecco's modified phosphate-buffered saline (PBS), without the cations Ca^{2+} and Mg^{2+}. The discs were then transferred to a 12-well cluster dish containing 2 ml of fresh RPMI 1640 medium. The discs were incubated at 29°C, on a platform rocker with 60° total deflection every 7.5 s over a 48-h period. The discs supporting the biofilms were gently rinsed with PBS for analysis.

Biofilm thickness and architecture. Forty-eight-hour biofilms were fixed with 2% (vol/vol) paraformaldehyde as previously described (35). After fixation and a PBS rinse, the biofilms were stained with calcofluor white M2R for cell wall chitin (Sigma-Aldrich). Biofilm thickness and architecture were analyzed as described previously with minor changes. Briefly, imaging was accomplished using a Bio-Rad 2100 two-photon laser scanning confocal microscope (LSCM) equipped with a Mai-Tai infrared laser (IR). Calcofluor white was excited with the IR laser at 780 nm, and emission was captured at 460 nm. A z-series of 500 scans were collected using the LaserSharp software (Bio-Rad). High-resolution z-stack images with an interval step of 0.25 μm were processed using Imaris 3D Image Processing & Analysis software (Bitplane). Orthogonal slices of ~100 μm were projected to afford a 90° pitch profile perspective. To assess the architecture of the midhyphal region, 20 scans were extracted from the middle of the stack and analyzed.

SEM. Biofilms were fixed in 2.5% glutaraldehyde in 0.1 M cacodylate buffer. After postfixation in 1% osmium, the biofilms were dehydrated through a graded ethanol series and further dehydrated by 50% hexamethyldisilazane (HMDS) followed by two rinses in 100% HMDS. The biofilms were allowed to air dry prior to sputter-coating with a 60:40 mixture of gold and palladium. The biofilms were viewed using a Hitachi S-4800 scanning electron microscope (SEM).

Adhesion assay. α-Pheromone-induced adhesion was assessed following incubation of 1 ml of white **a/a** cells at a concentration of 5×10^7/ml in fresh supplemented Lee's medium at 25°C in the wells of a Costar 12-well cluster plate (Corning Life Sciences) in the presence or absence of 3×10^{-6} M synthetic 13-mer α-pheromone with a sequence of GFRLTNFGYFEPG (Open Biosystems) according to methods previously published (33, 36). This pheromone has previously been demonstrated to induce the mating response in opaque cells of *C. dubliniensis* (16). The synthetic α-pheromone was dissolved in dimethyl sulfoxide (DMSO). For controls in the absence of pheromone, an equal amount of DMSO was added. After 16 h of incubation, the wells were washed gently with PBS. Adhesion was then quantified by releasing cells from the well bottoms using a 0.05% trypsin-EDTA solution (Invitrogen). The adherent cells were then counted with a hemocytometer. For comparative purposes, the means and standard deviations of three independent wells for each strain were calculated and presented in a bar chart. The adhesion experiment and all other experiments in this study were repeated at least twice, and similar results were obtained.

The **a**-pheromone-induced adhesion of α/α cells assay was performed in a similar fashion, except that instead of pheromone, 10% of an opaque cell mixture (1:1 **a/a** and α/α) was added to 90% white α/α test cells (44). The combination of majority white and minority opaque cells was then added to the wells of a Costar 12-well cluster plate and processed as described above.

Biofilm dry weight. White cell biofilms were generated without (−) and with (+) a 10% opaque cell mixture. After 48 h of incubation, the biofilms adhering to the silicone elastomer discs were washed in PBS. Biofilms were resuspended in a 0.05% trypsin-EDTA solution and transferred into 1.5 ml preweighed Seal Rite 1.5 Natural Microcentrifuge Tubes (USA Scientific). The samples were centrifuged (10 min, 14,000 rpm) and the supernatants discarded. The biofilm material was then desiccated us-

ing a SpeedVac Concentrator (Savant), and the preweighed tubes were weighed a second time to determine biofilm dry weight.

Hyphal and pseudohyphal vacuole imaging. Forty-eight-hour biofilms were briefly inverted onto a 20-μl droplet of water on a glass slide. Representative hyphae and pseudohyphae from the upper region of each biofilm were released into the water droplet. The water droplet was then dispersed by tapping a 22- by 60-mm coverslip over the droplet. Differential interference contrast (DIC) images were acquired using a Nikon TE2000 inverted microscope with an attached Canon EOS Rebel T3i digital camera.

RESULTS

Spontaneous switching from white to opaque. The white-opaque transition was originally discovered in the *C. albicans* α/α strain W0-1 (45) and subsequently demonstrated to occur in most natural *MTL*-homozygous strains within the employed thresholds of resolution (28). It was subsequently demonstrated to occur in *MTL*-homozygous strains of *C. dubliniensis* (16) and *Candida tropicalis* (46). Switching to the opaque phenotype by *MTL*-homozygous white cells is a requisite for mating competence of all three species (16, 29, 30, 46). *MTL*-homozygous cells switch spontaneously and reversibly between the white cell phenotype, which forms colonies that are white to light pink when grown on agar containing phloxine-B, and the opaque cell phenotype, which stains bright red on that agar (45). White appears to be the default phenotype, since deletion of the master switch gene, *WOR1*, blocks cells in the white phenotype (47–49). It was previously shown that 9 of 17 **a/a** strains and 6 of 10 α/α strains of *C. dubliniensis* underwent spontaneous switching (16), but a side-by-side comparison of variability between *C. albicans* and *C. dubliniensis* strains at the same stringency (1/1,000 to 10,000) was not performed. We therefore serially plated at high density (approximately 300 colonies per 10-cm plate) cells of 26 natural *MTL*-homozygous strains of *C. albicans* and 27 natural *MTL*-homozygous strains of *C. dubliniensis*. The origin and *MTL* configuration of the strains are presented in Table S1 in the supplemental material. Cells were plated on agar containing supplemented Lee's medium, and the plates were incubated for 7 days at 25°C in air. Switching in a strain was scored as the formation of one or more opaque colonies or white colonies with one or more opaque sectors among a total of approximately 15,000 colonies. We found that 85% of *C. albicans MTL*-homozygous strains and 56% of *C. dubliniensis MTL*-homozygous strains underwent the white-to-opaque transition, at the frequency threshold of $\geq 7 \times 10^{-5}$ (see Table S1 in the supplemental material). We then serially plated cells from opaque colonies or sectors of the two species in the same manner (>300 colonies per 10-cm plate) to assess the stability of the opaque phenotype in each species. Strains in which <10% of the plated opaque cells switched back to white were considered relatively stable for the opaque phenotype. Of the 22 strains of *C. albicans* that spontaneously switched from white to opaque, 21 (94%) exhibited opaque phase stability (see Table S1 in the supplemental material). Of the 15 strains of *C. dubliniensis* that switched from white to opaque, only 4 (27%) exhibited opaque phase stability (see Table S1 in the supplemental material).

To investigate further the decreased propensity of *MTL*-homozygous *C. dubliniensis* strains to switch from white to opaque and the increased propensity to switch from opaque back to white, we compared the switching frequencies of five *C. albicans* strains (12C, P34028, P37005, L26, P57072), randomly selected from the 22 strains that switched from white to opaque, with the five *MTL*-homozygous strains of *C. dubliniensis* with the most stable opaque phenotype assessed in the high-density plating experiments (d88014, d90006, d81217, d126423, ANSA5). White and opaque cells of each strain were plated at low density (approximately 30 to 60 colonies per 10-cm plate) on agar containing supplemented Lee's medium and were incubated for 7 days at 25°C in air. For the five random *C. albicans* strains, the frequency of white-to-opaque switching of two strains was $<10^{-4}$, while that of the remaining three were 4×10^{-4}, 9×10^{-4}, and 6×10^{-3} (Fig. 1A). The frequencies of white-to-opaque switching of the five *C. dubliniensis* strains were $<2 \times 10^{-4}$, $<4 \times 10^{-4}$, $<3 \times 10^{-4}$, $<2 \times 10^{-4}$, and $<2 \times 10^{-4}$ (Fig. 1A).

All *C. albicans* and *C. dubliniensis* strains switched from opaque to white at frequencies far higher than from white to opaque (Fig. 1A). Furthermore, *C. dubliniensis* strains switched from opaque to white at far higher frequencies than *C. albicans* strains (Fig. 1A). Of the five selected *C. albicans* strains, the frequency of switching from opaque back to white ranged from 6×10^{-3} to 4×10^{-1} (Fig. 1A). In marked contrast, the frequency of switching from opaque to white for *C. dubliniensis* strains ranged between 1.1×10^{-1} and 9.8×10^{-1} (Fig. 1A). The average frequency of opaque-to-white switching of the *C. dubliniensis* strains was 5×10^{-1}, while that of the *C. albicans* strains was 1.4×10^{-1}, a 3-fold difference.

In addition to a higher level of instability of the opaque phenotype, opaque phase cells of all five *MTL*-homozygous *C. dubliniensis* strains, when plated at low density, formed not only majority smooth white colonies at high frequencies, but also a minority of alternative (Alt) colony morphologies (Fig. 1D and 2B). These Alt colonies were irregular and mottled (Fig. 2B). None of the five *C. albicans* strains formed Alt colonies.

Variable opaque cell morphologies. In addition to instability of the opaque phase colony morphology, we had previously observed variability of the opaque cell phenotype within opaque colonies of a single *C. dubliniensis* strain (16). We therefore compared the uniformity of cellular phenotypes within individual white and opaque colonies among the five *MTL*-homozygous test strains of *C. albicans* and white, opaque, and Alt colonies of the five *MTL*-homozygous test strains of *C. dubliniensis*. Cells from single white (Wh) colonies of both the *C. albicans* and *C. dubliniensis* strains were equally round and relatively uniform in diameter (Fig. 2A and B, respectively). Although the shapes of opaque cells varied slightly between *C. albicans* strains, they were all at least twice as large as white cells and relatively uniform both in size and in shape for cells from individual colonies (Fig. 2A). This uniformity was not the case for cells from individual *C. dubliniensis* opaque colonies, which exhibited far more morphological variability and size heterogeneity than those of individual *C. albicans* colonies (Fig. 2B). Interestingly, cells from the Alt colonies of *C. dubliniensis* differed dramatically in shape and size between strains, including large and round (ANSA5, d88014), small and round (d90006), and small and elongate (d81217) (Fig. 2B), but the cell morphology within individual Alt colonies was uniform (Fig. 2B).

Loss of CO_2 induction. Huang et al. (50) demonstrated that high (20%) CO_2 induced white-to-opaque switching and stabilized the opaque phenotype in one strain of *C. albicans*. We therefore tested this response in the five *MTL*-homozygous test strains of *C. albicans* and the five *MTL*-homozygous test strains of *C. dubliniensis*. High CO_2 caused a dramatic increase in the frequency of switching from white to opaque in all five *C. albicans*

A. Air

White to opaque

C.albicans

Strain	*MTL* genotype	No. colonies	Switch frequency
12C	**a/a**	4620	$9x10^{-4}$
P34028	**a/a**	2923	$<3x10^{-4}$
P37005	**a/a**	2695	$4x10^{-4}$
L26	**a/a**	3155	$6x10^{-3}$
P57072	α/α	3498	$<3x10^{-4}$
Mean ± S.D.			$1.5 \pm 2.6x10^{-3}$

C.dubliniensis

Strain	*MTL* genotype	No. colonies	Switch frequency
d88014	**a/a**	4698	$<2x10^{-4}$
d90006	α/α	2366	$<4x10^{-4}$
d81217	**a/a**	3960	$<3x10^{-4}$
d126423	α/α	3388	$<2x10^{-4}$
ANSA5	α/α	4021	$<2x10^{-4}$
Mean			$<3x10^{-4}$

Opaque to white

C.albicans

Strain	*MTL* genotype	No. colonies	Switch frequency
12C	**a/a**	1215	$6x10^{-3}$
P34028	**a/a**	783	$9x10^{-3}$
P37005	**a/a**	855	$2x10^{-2}$
L26	**a/a**	1488	$4x10^{-1}$
P57072	α/α	996	$3x10^{-1}$
Mean ± S.D.			$1.4 \pm 1.9x10^{-1}$

C.dubliniensis

Strain	*MTL* genotype	No. colonies	Switch frequency
d88014	**a/a**	846	$9.8x10^{-1}$
d90006	α/α	1084	$2.2x10^{-1}$
d81217	**a/a**	913	$1.4x10^{-1}$
d126423	α/α	744	$1.1x10^{-1}$
ANSA5	α/α	504	$8.7x10^{-1}$
Mean ± S.D.			$4.6 \pm 4.3x10^{-1}$

B. 20% CO_2

White to opaque

C.albicans

Strain	*MTL* genotype	No. colonies	Switch frequency
12C	**a/a**	297	$10x10^{-1}$
P34028	**a/a**	196	$8x10^{-1}$
P37005	**a/a**	203	$9x10^{-1}$
L26	**a/a**	239	$10x10^{-1}$
P57072	α/α	217	$10x10^{-1}$
Mean ± S.D.			$9 \pm 1x10^{-1}$

C.dubliniensis

Strain	*MTL* genotype	No. colonies	Switch frequency
d88014	**a/a**	310	$<3x10^{-3}$
d90006	α/α	203	$<4x10^{-3}$
d81217	**a/a**	251	$<4x10^{-3}$
d126423	α/α	225	$<4x10^{-3}$
ANSA5	α/α	256	$8x10^{-3}$
Mean ± S.D.			$1.6 \pm 3.6x10^{-3}$

Opaque to white

C.albicans

Strain	*MTL* genotype	No. colonies	Switch frequency
12C	**a/a**	163	$<6x10^{-3}$
P34028	**a/a**	156	$<6x10^{-3}$
P37005	**a/a**	169	$<6x10^{-3}$
L26	**a/a**	215	$<5x10^{-3}$
P57072	α/α	174	$<6x10^{-3}$
Mean			$<6x10^{-3}$

C.dubliniensis

Strain	*MTL* genotype	No. colonies	Switch frequency
d88014	**a/a**	136	$5x10^{-2}$
d90006	α/α	162	$2x10^{-2}$
d81217	**a/a**	159	$4x10^{-2}$
d126423	α/α	117	$1x10^{-1}$
ANSA5	α/α	49	$3x10^{-1}$
Mean ± S.D.			$1 \pm 1x10^{-1}$

C. *C. albicans* (P37005)

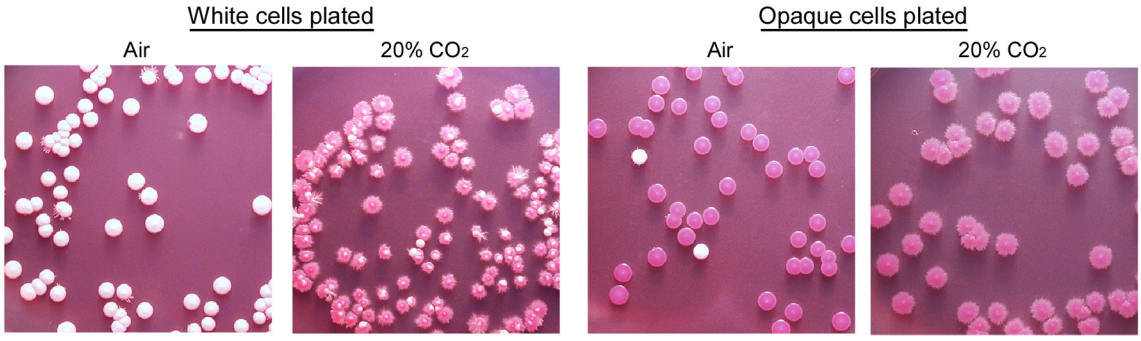

D. *C. dubliniensis* (ANSA5)

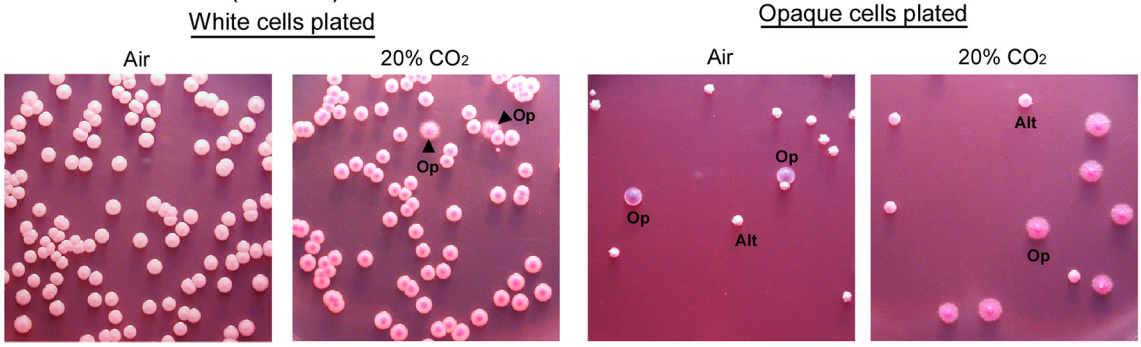

FIG 1 Strains of *Candida dubliniensis* switch from white to opaque at lower frequencies than strains of *Candida albicans* and exhibit opaque phase instability. (A) Frequencies of white to opaque and opaque to white in air for five randomly selected *C. albicans* strains and five *Candida dubliniensis* strains with the highest white-to-opaque switching frequencies. The former were randomly selected from 26 natural *MTL*-homozygous strains and the latter from 27 natural *MTL*-homozygous strains based on initial high-density plating experiments. The frequencies were obtained from low-density plating experiments (30 to 60 colonies per 10-cm plate). (B) Frequencies in 20% CO_2. Standard deviations were calculated for the data expressed in percentages and then converted to frequencies. The significance of the difference between the switching frequency (expressed as a percentage) distributions among *C. albicans* and *C. dubliniensis* strains was assessed by the nonparametric two-tailed Mann-Whitney test. In air, the differences observed were not significant. In contrast, in the presence of 20% CO_2, both white-to-opaque and opaque-to-white switching frequencies were significantly ($P < 0.05$) different between *C. albicans* and *C. dubliniensis*. (C) Morphologies and phloxine B staining of colonies of a representative *C. albicans* strain (P37005) grown in air or 20% CO_2. Opaque colonies are wider and stain red. (D) Morphologies and phloxine B staining of colonies of a representative *C. dubliniensis* strain (ANSA5) developed in air or 20% CO_2. Op, opaque colonies; Alt, alternative colonies.

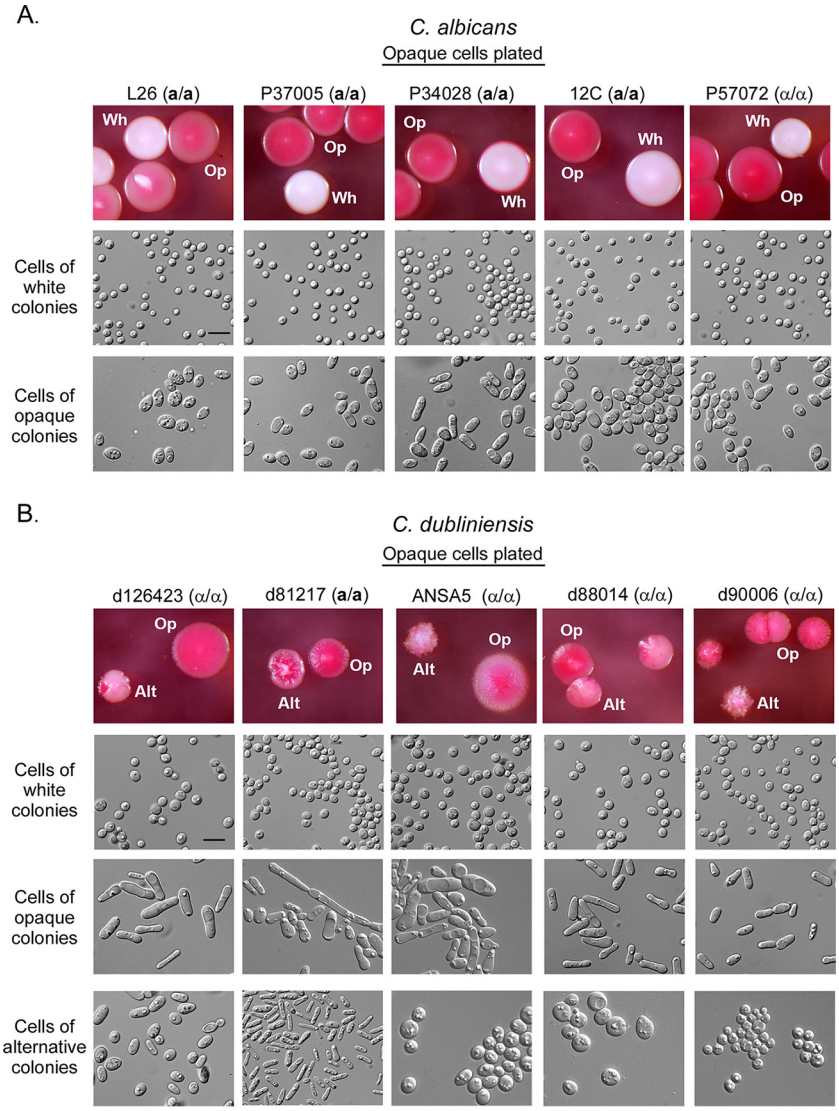

FIG 2 Opaque cells from opaque colonies of *C. dubliniensis*, but not *C. albicans*, exhibit intracolony heterogeneity. (A) Examples at high magnification of white and opaque colonies formed on low-density plates and the cell phenotypes within them, for five *MTL*-homozygous strains of *C. albicans*. (B) Examples at high magnification of white, opaque, and alternative colonies and the cell phenotypes within them, for five *MTL*-homozygous strains of *C. dubliniensis*. Op, opaque; Wh, white; Alt, alternative. Bars, 5 μm.

strains. The frequencies ranged from 75 to 100% (8×10^{-1} to 10×10^{-1}) (Fig. 1B). This represented a 660-fold increase over the average frequency in air. In marked contrast, the frequency of white-to-opaque switching in 20% CO_2 was undetectable in four of the five *C. dubliniensis* test strains ($<10^{-4}$; 8×10^{-3} for one strain, ANSA5). This represents an average negligible increase in frequency over that in air (1.2×10^{-3} and $<3 \times 10^{-4}$, respectively). These results indicate that *C. dubliniensis* either never possessed or lost this response.

To assess the stabilization of the opaque phenotype by CO_2 (50), opaque cells from opaque colonies obtained from high-density plating experiments (>300 colonies per plate) in air by the five test strains of each species, were plated at low density (~30 colonies per plate) and then immediately incubated in 20% CO_2 at 25°C for 7 days. For the five test strains of *C. albicans*, no detectable switching from opaque to white was observed ($<6 \times 10^{-3}$) (Fig. 1A). In marked contrast, the frequency of switching from opaque to white in the *C. dubliniensis* strains varied between 2 and 31% (2×10^{-2} to 3×10^{-1}) (Fig. 1A), close to the range of 11 to 98% (1×10^{-1} to 10×10^{-1}) observed in air (Fig. 1A). These results demonstrate that *C. dubliniensis* either never possessed or lost not only CO_2 induction of white-to-opaque switching but also CO_2 stabilization of the opaque phenotype.

Complex biofilm formation. In order for **a**/α cells of both *C. albicans* (29) and *C. dubliniensis* (16) to mate, they must first undergo homozygosis at the mating type locus (*MTL*) to **a/a** or α/α and then switch from the white to the opaque phenotype (Fig. 3A and B). In the formation of a biofilm by a homogeneous population of **a/a** white cells of *C. albicans*, in a modified version (34–36) of the model developed by Douglas and coworkers (51–53), minority opaque cells generated by spontaneous switching (~10^{-3} to 10^{-4}) release in an unorthodox fashion α-pheromone, which

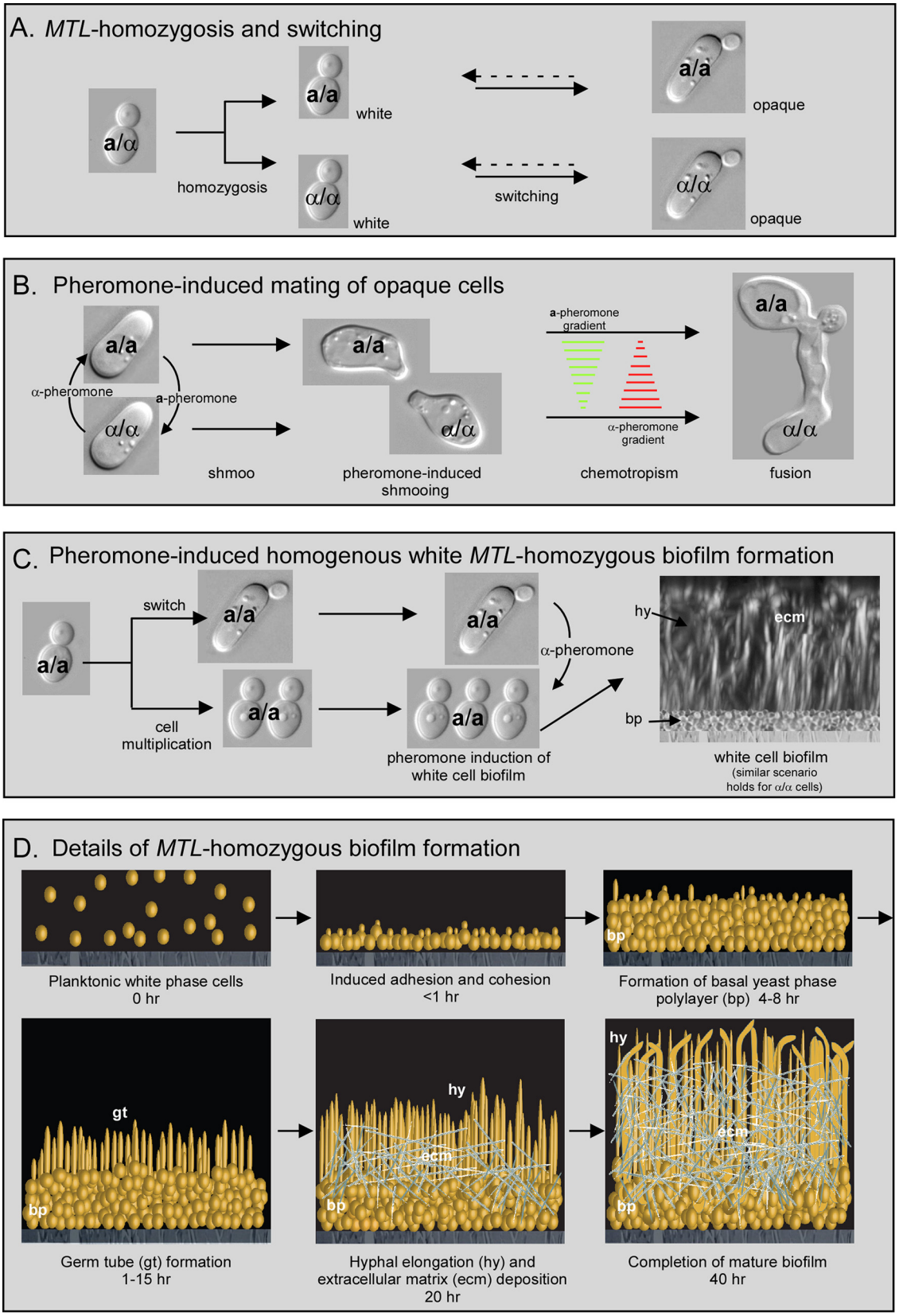

FIG 3 Steps in the process of biofilm formation leading from the *MTL* configuration **a**/α to **a/a** or α/α, in the formation of a *C. albicans MTL*-homozygous white cell biofilm. (A) *MTL* homozygosis, from the *MTL* **a**/α configuration to the **a/a** or α/α configuration of white cells, followed by the switch from white to opaque. (B) Pheromone-induced mating between opaque **a/a** and α/α cells. Green and red gradients of **a** and α pheromone direct mating tubes in the processes of chemotropism and fusion. (C) A paracrine system leads to white cell biofilm formation, in which, in the example here, a white **a/a** cell switches to the opaque phenotype, which then releases, in an unorthodox fashion, α-pheromone, which stimulates majority white **a/a** cell biofilm formation. (D) Changes in the cellular architecture in the *in vitro* formation of *MTL*-homozygous biofilms of *C. albicans* under the conditions of the Douglas model adapted by Daniels et al. (34, 35). The white threads at 20 and 40 h depict extracellular matrix. bp, basal yeast cell polylayer; gt, germ tubes; hy, hyphae; ECM, extracellular matrix.

stimulates majority **a/a** white cells to form a biofilm, in a paracrine induction system (Fig. 3C) (32). Addition of minority (10%) opaque cells (1:1, **a/a** and α/α) presumably serves to increase the level of α-pheromone and thus enhances the thickness of a mature **a/a** biofilm (34–36). In the process of generating complex **a**/α, and **a/a** or α/α, biofilms, planktonic cells are first grown to stationary phase in supplemented Lee's medium, which results in a uniform, unbudded population of planktonic yeast phase cells (39). These uniformly unbudded yeast phase cells are then diluted into RPMI 1640 medium buffered with MOPS (referred to here as RPMI medium) in the wells of a 12-well microtiter dish, with a silicone elastomer disc at the bottom, which serves as the substratum for biofilm development (34–36). The originally planktonic yeast cells settle and adhere to the disc in 1 h. In this model, adhering cells then form a basal yeast cell polylayer through cell multiplication over a 4- to 8-h period (Fig. 3D). Cells at the distal top edge of the basal layer then form germ tubes, which grow into true hyphae (Fig. 3D). As the hyphae elongate, they orient vertically, depositing an extracellular matrix (ECM) (Fig. 3D). After 48 h at 29°C or 37°C, in air or 20% CO_2, the basal layer constitutes approximately 20%, and the upper hypha-ECM layer 80%, of the biofilm volume (34, 35). This scenario (Fig. 3D) holds for homogeneous populations of *MTL*-heterozygous (**a**/α) cells and *MTL*-homozygous (**a/a**, α/α or **a/a** plus α/α) cells and for white cell populations to which 10% opaque cells have been added to stimulate thickness.

Biofilm formation by *MTL*-heterozygous strains. Using this model, biofilm formation was first compared between a collection of three **a**/α *C. albicans* strains and a collection of six **a**/α *C. dubliniensis* strains. The three *C. albicans* **a**/α test strains formed biofilms with thicknesses ranging between 74 and 78 μm, with a mean ± standard deviation of 76 ± 4 μm (Table 1). All three formed a basal yeast cell polylayer and then an upper region of vertically oriented hyphae encapsulated in ECM (Table 1). In Fig. 4A, a side view of a laser scanning confocal microscope (LSCM) projection image, generated with 500 stacked scans through 125 μm of a calcofluor white-stained biofilm formed by the representative *C. albicans* **a**/α strain SC5314, is presented; in Fig. 4B, a scanning electron microscopic (SEM) image of the top view of the hyphal upper region of the biofilm is shown; and in Fig. 4C, an architectural model deduced by examining the individual LSCM scans in the *z* axis is presented. ECM density was evaluated by increasing brightness, which revealed diffuse staining between the intensely stained hyphae. The upper region of vertical hyphae was affirmed by examining a limited set of 20 LSCM scans halfway through the biofilm (Fig. 5A). The pattern was punctate, indicating the vertical orientation of hyphae (34). The SEM top view of this biofilm (Fig. 4B) revealed the uniformity of the dominating true hyphal phenotype and absence of yeast cell pockets in the upper region, but fixing for SEM does not preserve the vertical orientation of the hyphae.

The six **a**/α *C. dubliniensis* test strains formed biofilms with thicknesses ranging from 39 to 58 μm, with a mean ± standard deviation of 46 ± 9 μm, approximately 40% less on average than the mean thickness of the *C. albicans* **a**/α biofilms (Table 1). Four of the six formed a basal yeast cell polylayer (Table 1). Two of the six (d11, d930953) formed a thick pseudohyphal upper region without a basal yeast cell polylayer, and three (d930664, d930822, d930936) formed a basal yeast cell polylayer and thick upper region of pseudohyphae (Table 1). The pseudohyphae in the five last biofilms were not vertically oriented but rather formed a tangled mesh, as is evident in the LSCM scans in the middle of the d11 biofilm (Fig. 5B). There was a noticeable reduction in ECM density in the pseudohyphal biofilms of all five of these strains (Table 1). In the biofilms of two of these strains, the basal yeast cell polylayer also contained minority pseudohyphae and hyphae. A side view of an LSCM projection image of the biofilm of *C. dubliniensis* **a**/α strain d11 is presented in Fig. 4D; a top view of the pseudohyphae obtained by SEM is presented in Fig. 4E; and the deduced architectural model is presented in Fig. 4F. Only one *C. dubliniensis* **a**/α strain, B71507, formed both a basal yeast cell polylayer and an upper region of pseudohyphal patches mixed with vertically oriented hyphae encapsulated in extracellular matrix (Table 1). Intermediate LSCM scans revealed a pattern both punctate and clumped, indicative of a mixture of pseudohyphal patches and vertically oriented hyphae (Fig. 5C). Because B71507 was the only strain that formed vertically oriented hyphae, it was genetically reaffirmed as *C. dubliniensis* by performing the PCR for 25S rRNA and *HWP1* (Fig. 6A and B, respectively). These results revealed that unlike the uniform biofilms of *C. albicans*, the biofilms of *C. dubliniensis* **a**/α strains were architecturally variable and dominated by pseudohyphae. One strain, B71507, however, formed a biofilm that exhibited some of the architectural features of a *C. albicans* **a**/α biofilm. It should be noted that the biofilms that did not contain a uniform basal layer of yeast cell polylayer (d11, d930953) were composed of yeast cells plus pseudohyphae (Table 1).

Pheromone-induced adhesion. Pheromone of opposite mating types has been shown to induce adhesiveness of *MTL*-homozygous white cells (33, 36, 37) and is believed to play a role in establishing the initial yeast cell monolayer on the substratum, the initial step in biofilm formation *in vitro* (Fig. 3D). We therefore tested whether the addition of α-pheromone to planktonic white **a/a** cells of *C. dubliniensis* strains or the addition of 10% opaque cells (50% **a/a,** 50% α/α), a source of **a**-pheromone, to planktonic white *C. dubliniensis* α/α cell strains, induced adhesion.

For every one of the 10 *MTL*-homozygous strains of *C. albicans* tested and every one of the 15 *MTL*-homozygous strains of *C. dubliniensis* tested, incubation for 16 h with either pheromone for **a/a** white cells or 10% opaque cells for α/α white cells resulted on average in a >100-fold increase in adhesion to tissue culture dish bottoms (Fig. 7A and B, respectively). The mean number of adhering cells per well bottom for induced *C. albicans* and *C. dubliniensis* strains was 1.8×10^8 and 1.6×10^8, respectively (Fig. 7A and B). The variability of induction among strains was reflected by the standard deviations, which were 0.5×10^6 for the set of strains of both species, representing 28% and 31% of the mean, respectively (Fig. 7A and B). Therefore, the average level of induction of adhesion and the variability among strains of *C. dubliniensis* were similar to those of *C. albicans*.

Biofilm formation by *MTL*-homozygous strains. To compare biofilm formation and the architectures of *MTL*-homozygous *C. albicans* and *C. dubliniensis* biofilms, 12 strains of the former and 8 strains of the latter were analyzed by LSCM. All six **a/a** and six α/α strains of *C. albicans* formed biofilms, which after 48 h of development contained a basal yeast cell polylayer and an upper layer of vertically oriented hyphae encased in ECM (Table 1). A side view of an LSCM projection image of a representative biofilm of a *C. albicans* **a/a** strain, P37005, is presented in Fig. 4G, a top view of hyphae in the upper region obtained by SEM is presented in Fig. 4H, and the architectural model, deduced by individually

TABLE 1 Comparison of biofilm formation of *MTL*-heterozygous (**a**/α) strains of *Candida albicans* and *Candida dubliniensis* and *MTL*-homozygous (**a/a** or α/α) strains of the two species[a]

Species (*MTL* zygosity)	*MTL* configuration	Strain	Biofilm thickness (μm)[b]	Yeast cell basal layer	Hyphal upper layer	Vertical orientation of hyphae	Pseudohyphae	Extracellular matrix
C. albicans (heterozygous)	**a**/α	SC5314	78 ± 5	++++	++++	++++	−	++++
		P37039	76 ± 2	++++	++++	++++	−	++++
		P37037	74 ± 3	++++	++++	++++	−	++++
			76 ± 4					
C. albicans (homozygous)	**a/a**	P37037	51 ± 3	++++	++++	++++	−	++++
		P37005	57 ± 5	++++	++++	++++	−	++++
		P37039	57 ± 2	++++	++++	++++	−	++++
		P34028	56 ± 2	++++	++++	++++	−	++++
		12C	56 ± 2	++++	++++	++++	−	++++
		L26	58 ± 1	++++	++++	++++	−	++++
			56 ± 3					
	α/α	WO-1	58 ± 3	++++	++++	++++	−	++++
		P37037	61 ± 4	++++	++++	++++	−	++++
		P37039	56 ± 2	++++	++++	++++	−	++++
		P57072	57 ± 2	++++	++++	++++	−	++++
		GC75	60 ± 1	++++	++++	++++	−	++++
		19F	57 ± 1	++++	++++	++++	−	++++
			58 ± 2					
C. dubliniensis (heterozygous)	**a**/α	d11	39 ± 6	−[c]	−	−	++++	+
		d930953	41 ± 2	−[c,e]	−	−	++++	+
		B71507	58 ± 4	+++	+++	+++	++	+++
		d930664	55 ± 4	++++	−	−	++++	+
		d930822	45 ± 3	+++[c]	−	−	++++	+
		d930936	40 ± 3	+++[d]	−	−	+++	+
			46 ± 9					
C. dubliniensis (homozygous)	**a/a**	d88014	47 ± 4	+++[c]	−	−	++++	+
		UP16	37 ± 1	+++[d]	+	−	+++	+
		d81217	32 ± 2	+++	−	−	−	+
		UP29	36 ± 2	+++	−	−	++	+
			38 ± 6					
	α/α	ANSA5	33 ± 5	++[d]	−	−	+++	+
		ANSA28	38 ± 2	+++	−	−	+	+
		d126423	35 ± 2	++++	−	−	+	+
		P86	39 ± 1	+++	+	−	++	+
			36.3 ± 3					

[a] Symbols: ++++, +++, ++, +, level of traits relative to SC5314 (++++) for **a/α** strains and P37037 (++++) for **a/a** and α/α strains. − indicates trait is absent.
[b] Values in boldface indicate the average and standard deviation for the set of strains listed immediately above.
[c] Basal layer contains predominately pseudohyphae and minority yeast phase cells.
[d] Basal layer contains yeast phase cells, pseudohyphae, and hyphae.
[e] Basal layer is patchy or fragmented.

analyzing the 500 LSCM scans, is presented in Fig. 4I. Except for thickness, the architecture of white **a/a** biofilms was similar to that of **a**/α biofilms of *C. albicans* (Table 1). Note that the SEM revealed true hyphae with no yeast phase cell pockets (Fig. 4H), as did the SEM of the representative biofilm of the **a**/α *C. albicans* strains SC5314 (Fig. 4B).

All four **a/a** and all four α/α strains of *C. dubliniensis* formed a basal yeast cell polylayer, although they were not as uniformly thick among strains as those of *C. albicans* **a/a** and α/α strains (Table 1). The basal yeast cell polylayers of three strains contained pseudohyphae and hyphae among the yeast cells (Table 1). None of the biofilms of the eight *MTL*-homozygous *C. dubliniensis* strains formed a thick, uniform upper layer of vertically oriented hyphae. Three strains formed a thick upper mesh of pseudohyphae, two a reduced upper layer of pseudohyphae, two an upper layer containing an intermediate amount of pseudohyphae, and one, d81217 (**a/a**), no upper layer of either hyphae or pseudohyphae (Table 1). The biofilm of the last strain consisted entirely of a basal yeast cell polylayer (Table 1). All of these *MTL*-homozygous strains appeared to contain reduced ECM (Table 1). A side view of an LSCM projection image of the biofilm and of strain d88014 (**a/a**), an SEM of the pseudohyphae in the upper region, and the architectural model deduced by individually analyzing the 500 LSCM scans are presented in Fig. 4J, K, and L, respectively. Note that the upper layer was uniformly composed of pseudohyphae (Fig. 4K).

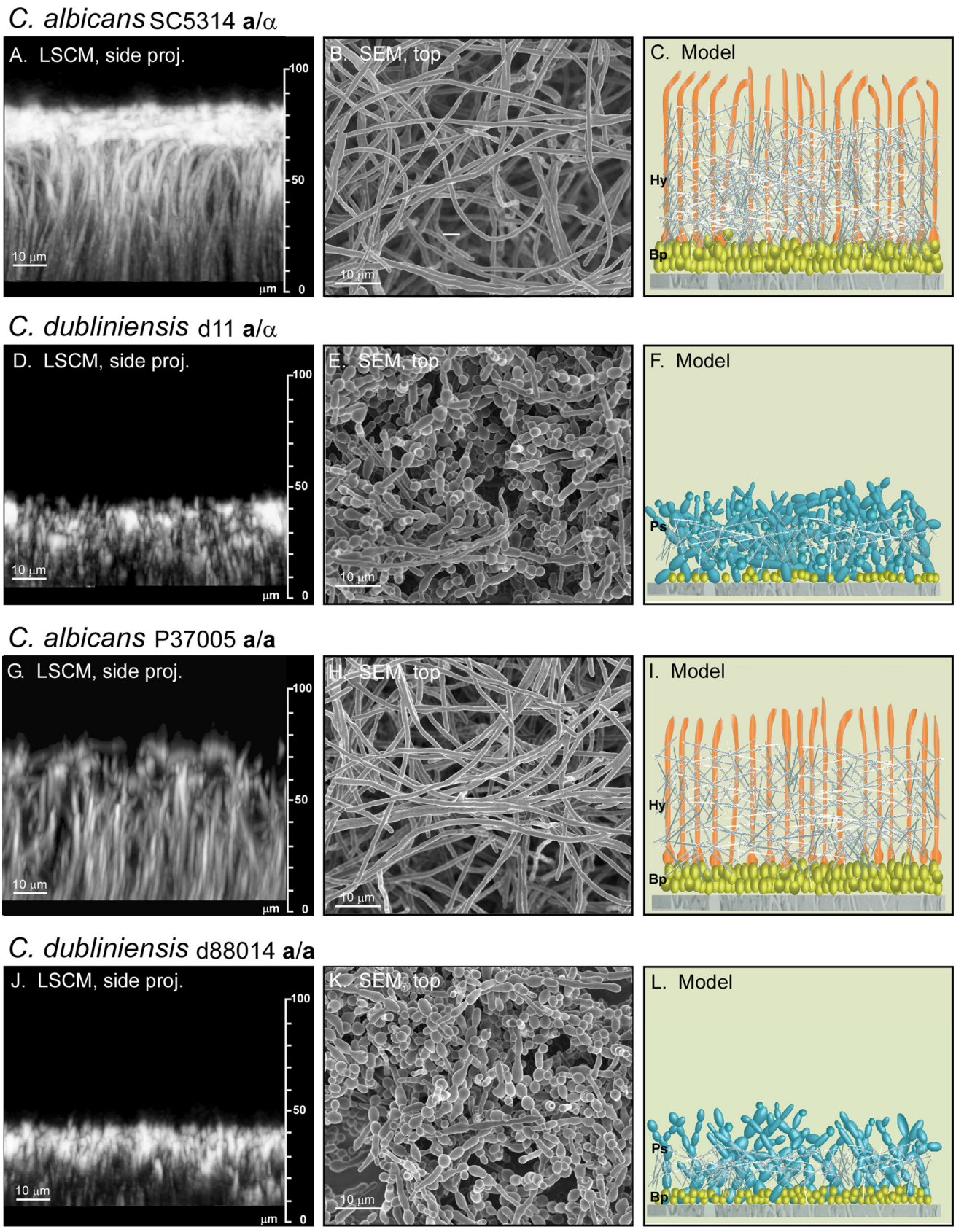

FIG 4 Comparison of the cellular architecture of *MTL*-heterozygous and *MTL*-homozygous *C. albicans* and *C. dubliniensis* biofilms. (A, D, G, J) Side views of projection images of laser scanning confocal microscopy stacks of 500 scans of calcofluor white-stained 48-h biofilms of representative strains of **a**/α and **a/a** biofilms of *C. albicans* and *C. dubliniensis*. (B, E, H, K) Scanning electron microscopy images (top view) of 48-h biofilms. Note the dominance of true hyphae in the *C. albicans* **a**/α and **a/a** biofilms and the dominance of pseudohyphae in the *C. dubliniensis* **a**/α and **a/a** biofilms. (C, F, I, L) Models of biofilm architecture deduced by examining individual LSCM scans in the stacks of 500 scans each. The white threads represent extracellular matrix. Bp, basal yeast cell polylayer (yellow); Hy, true hyphae (orange); Ps, pseudohyphae (blue). Scale bars, 10 μm.

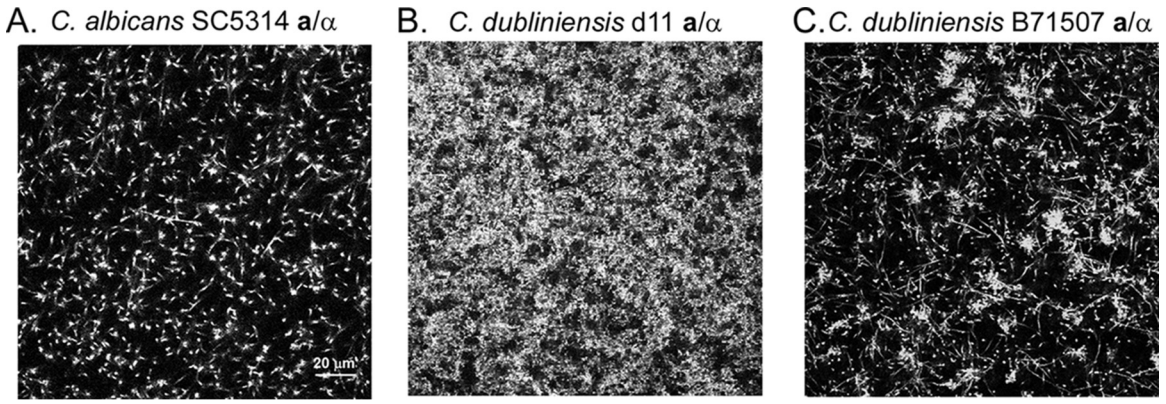

FIG 5 Architecture of hyphae and pseudohyphae of representative 48-h biofilms, revealed by viewing from the top LSCM scans extracted from the middle of the 500 scans taken through the entire biofilm. (A) *C. albicans* **a**/α strain SC5314. Note that the punctate pattern suggests that the hyphae in the middle of the biofilm are vertically oriented. (B) *C. dubliniensis* **a**/α strain d11. Note the mesh of pseudohyphae, with no directionality. (C) *C. dubliniensis* **a**/α strain B71507. Note that this particular strain forms a biofilm that contains both punctate hyphal areas and patches of pseudohyphae. Scale bar, 20 μm.

***MTL*-homozygous biofilm thickness and mass.** Measurements of thickness using side views of LSCM projection images (e.g., Fig. 4A, D, G, and J) revealed a significant difference between biofilms formed by white cells of *MTL*-homozygous strains of *C. albicans* and by those of *C. dubliniensis*. The mean thickness of the 12 *C. albicans MTL*-homozygous biofilms was 57 ± 3 μm, 25% less than that of *C. albicans* **a**/α biofilms (*P* value < 0.05) (Table 1), a difference previously reported (32). The mean thickness (± standard deviation) of biofilms formed by the eight *MTL*-homozygous *C. dubliniensis* strains was 37 ± 5 μm, 19% less than *C. dubliniensis* **a**/α biofilms (*P* value < 0.05) and 35% less than *C. albicans MTL*-homozygous biofilms (*P* value < 0.05) (Table 1). However, even though the thickness of *MTL*-homozygous white cell biofilms of *C. dubliniensis* was less than that of *C. albicans*, the mean dry weight of the two were statistically indistinguishable. The mean dry weights of 10 *MTL*-homozygous *C. albicans* and 15 *MTL*-homozygous *C. dubliniensis* biofilms were 0.75 ± 0.13 and 0.67 ± 0.29 mg per biofilm, respectively (Fig. 7C and D, respectively). The difference was not significant (*P* value > 0.05). There was more variability among the *C. dubliniensis* strains than among the *C. albicans* strains, as indicated by the standard deviation, which was more than twice as large for *C. dubliniensis* (Fig. 7C and D, respectively).

Minority opaque cell stimulation. We previously showed that the addition of minority (10%) opaque cells (one-half **a/a** and one-half α/α) to majority (90%) white **a/a** or α/α cells of *C. albicans* stimulates an increase in biofilm thickness, presumably because the added opaque cells secrete pheromone (32–34, 36, 54). We also showed previously that the addition of minority opaque cells to majority white cells did not affect the general architecture of the biofilm that formed. Stimulated biofilms still consisted of a basal yeast cell polylayer and an upper region of vertical hyphae embedded in an extracellular matrix (34, 36). We therefore tested whether the addition of minority opaque cells stimulated the thickness and/or architecture of biofilms formed by majority white cells of *C. dubliniensis*. The addition of minority *C. albicans* opaque cells to white cells of five test strains of *C. albicans* stimulated biofilm thickness by between 23 and 33%, with a mean ±

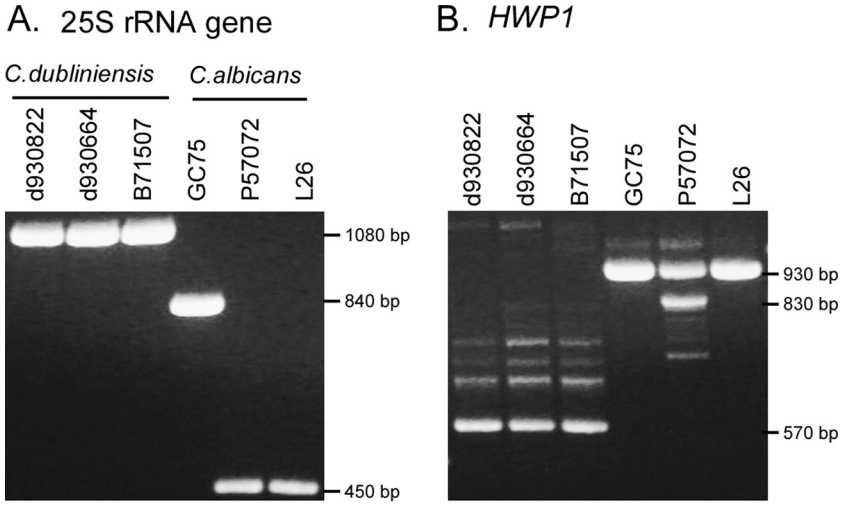

FIG 6 Verification that strain B71507, which is the only *C. dubliniensis* strain to contain vertically oriented hyphae in a 48-h biofilm, is in fact of that species by PCR. Discrimination was based on the size polymorphism of the intron of the 25S rRNA gene and of the *HWP1* gene.

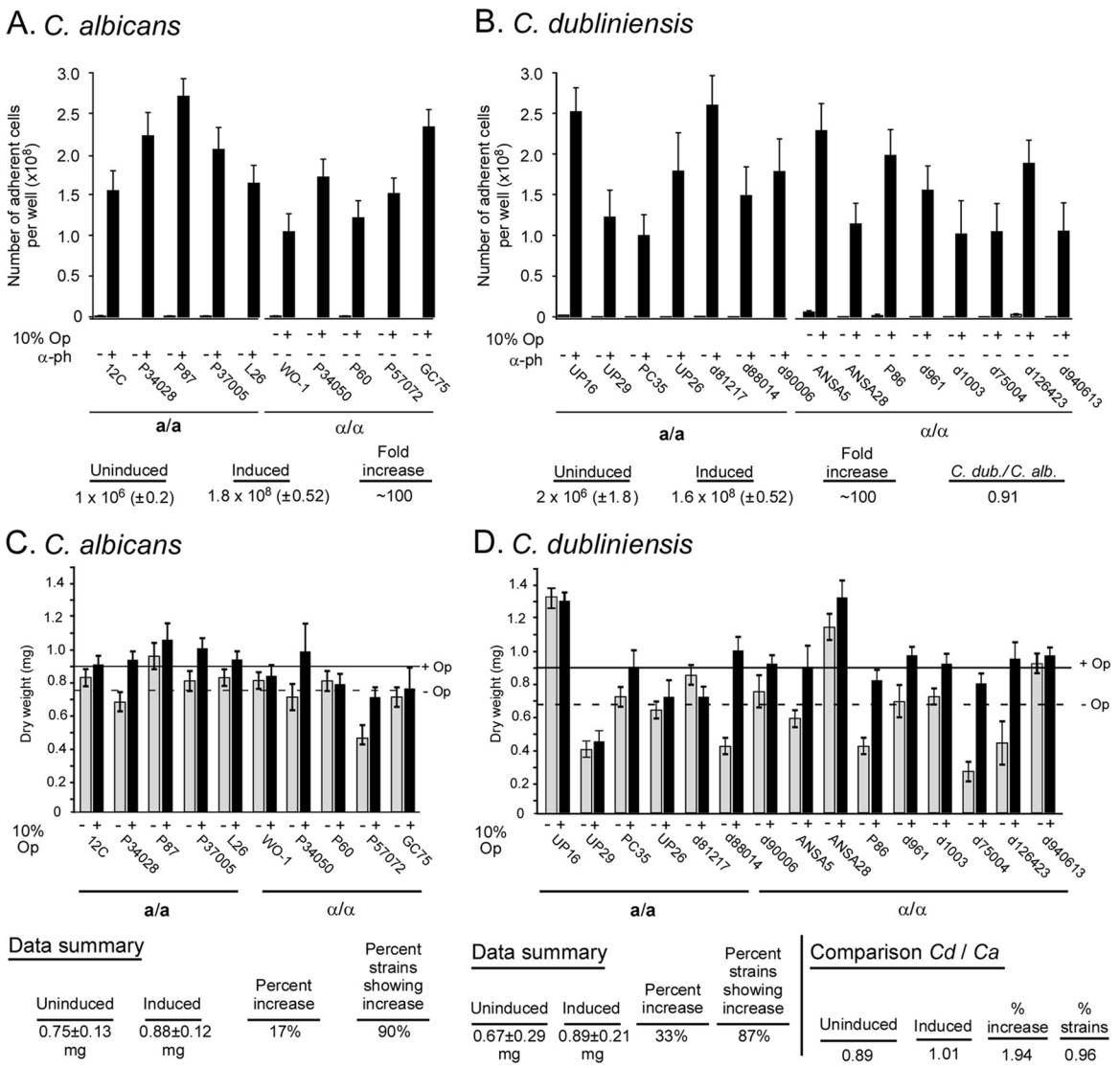

FIG 7 The variability of α-pheromone (or minority opaque cell) stimulation of adhesion and the variability of unstimulated and minority opaque cell-stimulated dry weight of white *MTL*-homozygous biofilms are similar among strains of *C. albicans* and *C. dubliniensis*. (A and B) α-Pheromone or minority (10%) opaque cell (1:1, *C. albicans* **a/a** and α/α) stimulation of adhesion to tissue culture plastic of **a/a** and α/α planktonic cells, respectively, of *C. albicans* and *C. dubliniensis* strains. The means ± standard deviations of uninduced and induced adherent cells per well and the fold increases due to induction are presented at the bottom of panels. (C and D) Minority opaque cell stimulation of dry weight for 48-h **a/a** and α/α biofilms of *C. albicans* and *C. dubliniensis*, respectively. The solid or dashed horizontal lines represent the means in the presence or absence, respectively, of minority opaque cells. A data summary of the means ± standard deviations of uninduced and induced dry weights, percent increases due to induction, and percentages of strains induced are presented at the bottom of the panels. − α ph, no α pheromone added; + α ph, α pheromone added; − Op, no addition of 10% opaque cells; + Op, addition of 10% opaque cells.

standard deviation of 28% ± 4% (Table 2). Stimulation in all strains had no effect upon biofilm architecture (Table 2). In the case of *C. dubliniensis*, the addition of minority *C. dubliniensis* opaque cells (one-half **a/a** and one-half α/α) to majority white cells stimulated thickness in the three tested strains between 17 and 31%, with a mean ± standard deviation of 22% ± 8% (Table 2). The addition of minority *C. albicans* opaque cells caused a much larger increase in thickness than did the addition of minority *C. dubliniensis* opaque cells. *C. albicans* opaque cells stimulated thickness between 37 and 59%, with a mean ± standard deviation of 46% ± 11%, over twice the impact of minority *C. dubliniensis* opaque cells (Table 2). The impact of minority opaque cells on dry weight was also compared between the two species, but in this case only for stimulation by 10% *C. albicans* opaque cells. For *C. albicans*, the mean stimulation of the dry weight of 10 strains was 17% (Fig. 7C), while that of 15 *C. dubliniensis* strains was 33% (Fig. 7D).

In spite of the significant difference between pheromone-stimulated *C. albicans* and *C. dubliniensis* in mean thickness (Table 2), the mean dry weight of the two were statistically indistinguishable (0.88 ± 0.12 mg per biofilm and 0.89 ± 0.21 mg per biofilm, respectively [Fig. 7C and D, respectively]). Finally, the architecture of *MTL*-homozygous *C. dubliniensis* biofilms stimulated with minority *C. dubliniensis* or *C. albicans* opaque cells was examined in the three strains by LSCM. Minority *C. dubliniensis* opaque cells had no effects on the basal yeast cell polylayer, but minority *C.*

albicans opaque cells caused an increase (Table 2). In all three strains, both minority *C. dubliniensis* and *C. albicans* opaque cells stimulated a low level of hypha formation, in two cases with small patches of vertically orientated hyphae (Table 2). However, in no strain did minority opaque cells of either species stimulate a uniform upper region of vertically oriented hyphae embedded in a dense ECM (Table 2). In the case of *C. dubliniensis* strain d81217, which when unstimulated did not form an upper region of pseudohyphae, minority opaque cells of both species stimulated an upper layer of pseudohyphae.

Explaining the mass-volume contradiction. The significant difference in mean thickness but the similarity in mean dry weight between *C. albicans* and *C. dubliniensis* biofilms, either unstimulated or pheromone stimulated, presented a conundrum. This may be explained in part by the difference in cytoplasmic density between hyphae and pseudohyphae, revealed by differential interference contrast microscopy. While the cellular compartments of true hyphae in *C. albicans* biofilm were dominated by a sequence of vacuoles with aqueous, particulate-free interiors (Fig. 8A and B), the compartments of the pseudohyphae of *C. dubliniensis* biofilms contained roughly one-half of the number of vacuoles and contained a far greater proportion of particulate cytoplasm (Fig. 8C and D). An additional explanation may be that the pseudohyphal mesh formed in biofilms of *MTL*-homozygous *C. dubliniensis* cells appears to be more compact, containing more cell compartments per unit volume than the vertically oriented, nonbranching hyphae in *C. albicans* biofilms (compare Fig. 4H and K and Fig. 4I and L). Although *C. albicans* biofilms contain far more ECM than *C. dubliniensis* biofilms (Tables 1 and 2), the collapse of ECM during dehydration procedures suggests that it has a very high water content. Hence, although the *C. albicans* biofilm is significantly thicker, it may contain more fluid in the extracellular space.

DISCUSSION

Sequencing of the genome of *C. dubliniensis* revealed that it was highly similar to that of *C. albicans*, with a high degree of synteny (13). Furthermore, sequencing revealed that in *C. albicans*, but not in *C. dubliniensis*, there has been an expansion of gene families implicated in pathogenesis (13) and 168 species-specific genes. Moreover, Moran et al. (23) reviewed evidence suggesting that *C. dubliniensis* is undergoing reductive evolution (55), in part through pseudogenization and gene loss. It has been suggested (8) that the failure to expand specific gene families and reductive evolution are the reasons why *C. dubliniensis* is isolated far less frequently than *C. albicans* (56), rarely causes bloodstream candidemias (27, 57), and is less virulent in animal models than *C. albicans* (15, 19, 20, 58). It had also been demonstrated prior to sequencing of the *C. dubliniensis* genome that genomic reorganization occurred at an extremely high frequency in *C. dubliniensis* compared to *C. albicans*, leading to highly unstable karyotypes (24–26). Indeed, in a DNA fingerprinting analysis of 10 strains of *C. dubliniensis* using three different midrepeat sequence probes specific for *C. dubliniensis*, no two isolates exhibited the same or even similar Southern blot hybridization patterns (24). Furthermore, hybridization of the contour-clamped homogeneous electric field (CHEF)-separated chromosomes of three strains with these probes or staining with ethidium bromide gave three distinct strain-specific patterns (24). Magee et al. (26) found different CHEF karyotypes for seven additional strains of *C. dubliniensis*.

TABLE 2 Effects on biofilm of adding minority opaque cells to majority white cells of *Candida albicans* and *Candida dubliniensis*[a]

Species	Majority white cell strain (zygosity)	Upper biofilm zone							Extracellular matrix
		Addition of 10% opaque cells	Opaque cell species	Avg biofilm thickness ± SD (μm)	% inducted thickness	Yeast cell basal layer	Hyphal upper layer	Vertical orientation of hyphae	Pseudohyphae	
C. albicans	P37037 (**a/a**)	No	–	51 ± 3		++++	++++	++++	–	++++
		Yes	*C. albicans*	68 ± 8	33	++++	++++	++++	–	++++
	P37005 (**a/a**)	No	–	57 ± 5		++++	++++	++++	–	++++
		Yes	*C. albicans*	72 ± 6	26	++++	++++	++++	–	++++
	P37039 (**a/a**)	No	–	57 ± 2		++++	++++	++++	–	++++
		Yes	*C. albicans*	70 ± 1	23	++++	++++	++++	–	++++
	P37037 (α/α)	No	–	61 ± 4		++++	++++	++++	–	++++
		Yes	*C. albicans*	81 ± 5	33	++++	++++	++++	–	++++
	P37039 (α/α)	No	–	56 ± 2		++++	++++	++++	–	++++
		Yes	*C. albicans*	71 ± 2	27	++++	++++	++++	–	++++
C. dubliniensis	d81217 (**a/a**)	No	–	32 ± 2		+++	–	–	–	+
		Yes	*C. dubliniensis*	42 ± 2	31	++++	++	–	++	++++
		Yes	*C. albicans*	51 ± 2	59	++++	++	+	++	++++
	ANSA5 (α/α)	No	–	38 ± 2		++	–	–	++	+
		Yes	*C. dubliniensis*	45 ± 1	18	++	++	–	++	–
		Yes	*C. albicans*	55 ± 2	44	++++	++	–	++	++
	d126423 (α/α)	No	–	35 ± 2		++++	–	–	+	+
		Yes	*C. dubliniensis*	41 ± 1	17	++	+	–	–	–
		Yes	*C. albicans*	48 ± 2	37	++++	++	++	++	++

[a] Symbols: ++++, +++, ++, +, level of traits to relative to P37037 (**a/a**). – indicates trait is absent.

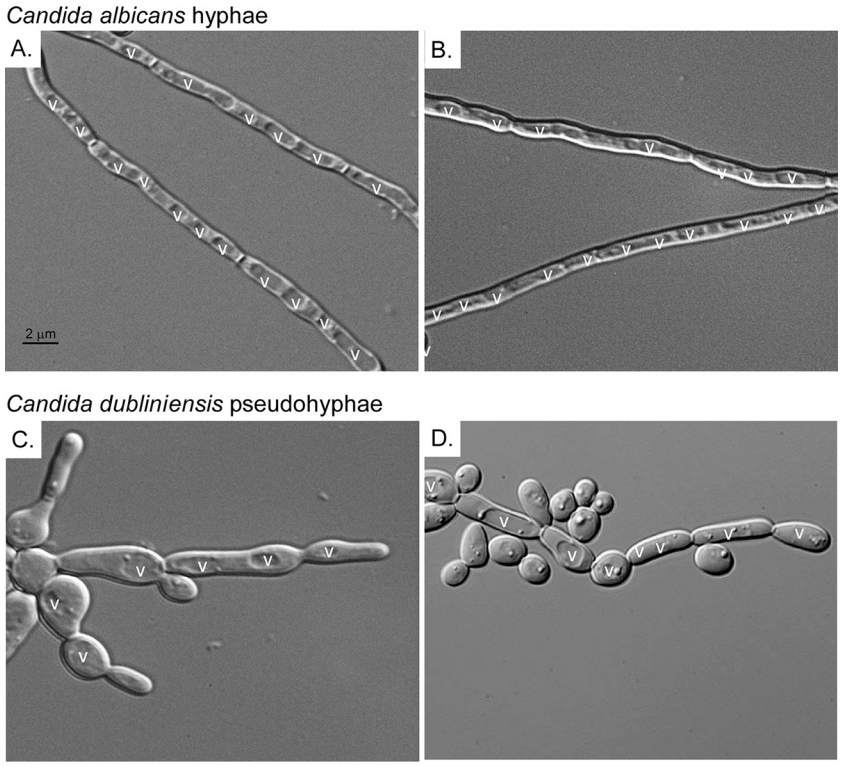

FIG 8 The higher degree of vacuolization of *C. albicans* hyphae and the greater proportion of nonvacuolar cytoplasm in *C. dubliniensis* pseudohyphae may account in part for the observation that although 48-h hypha-dominated *C. albicans* biofilms are thicker than 48-h pseudohypha-dominated *C. dubliniensis* biofilms, the two have similar mean dry weights. V, vacuole. Scale bar, 2 μm.

Joly et al. (25) presented evidence that changes occurred in part as a result of the reorganization of the repeat sequence RPS, found in *C. albicans* as well as *C. dubliniensis*. They suggested that RPS clusters functioned as recombination hot spots and that the higher rate of reorganization in *C. dubliniensis* was due in part to the observation that *C. dubliniensis*, on average, has approximately 2.5 times as many RPS units as *C. albicans*. Reorganization at RPS clusters was shown to occur in one strain after only 200 generations (25). This high level of genomic instability in *C. dubliniensis* may explain the higher level of variability and the deterioration of complex developmental programs, such as hypha formation (14, 15).

However, there is one additional factor that is rarely considered in studies of strain variability in *C. dubliniensis*, namely, the configuration of the *MTL* locus. Pujol et al. (16) found in an analysis of 82 *C. dubliniensis* isolates that 27 (33%) were homozygous at the *MTL* locus (**a/a** or α/α). Several previous studies of *C. albicans* (27, 28, 59) found that <10% of clinical isolates were *MTL* homozygous. In the most thorough of these studies (27), 110 (8.5%) of 1,294 *C. albicans* isolates were found to be *MTL* homozygous. The reason that the configuration of the *MTL* locus represents an important issue that should not be overlooked in studies of *C. dubliniensis* is that *MTL*-heterozygous and *MTL*-homozygous cells have been shown to differ phenotypically in *C. albicans*. In *C. albicans*, *MTL*-homozygous cells are able to undergo white-opaque switching, whereas *MTL*-heterozygous cells are not (28, 29); and *MTL*-homozygous cells are able to mate, whereas *MTL*-heterozygous cells are not (29, 30). *MTL*-homozygous cells form biofilms that are functionally different from those formed in *MTL*-heterozygous cells (31–33). While *MTL*-heterozygous biofilms are impenetrable by human white blood cells and impermeable to both low- and high-molecular-weight molecules, *MTL*-homozygous biofilms are both permeable and penetrable (32, 35, 60, 61). While *MTL*-homozygous cells respond to pheromone by activating the mitogen-activated protein (MAP) kinase pathway to form a biofilm, *MTL*-heterozygous cells do not (32, 33). While *MTL*-homozygous cells treated with pheromone acquire adhesivity and upregulate genes associated with the MAP-kinase pathway, *MTL*-heterozygous cells do not (32, 34–37; results presented here). Planktonic *MTL*-homozygous cells are on average less susceptible than *MTL*-heterozygous cells to fluconazole (42% versus 5%), itraconazole (21% versus 4%), voriconazole (17% versus 2%), and flucytosine (25% versus 10%) (27). And finally, while cells within an *MTL*-heterozygous biofilm are relatively resistant to fluconazole, cells in *MTL*-homozygous biofilms are more susceptible (32–35, 54). It therefore may be less of an issue in studies of *C. albicans* to verify the configuration of the *MTL* locus, because only 5 to 10% of strains are *MTL* homozygous, but it is a major issue for *C. dubliniensis*, in which one in every three strains is *MTL* homozygous. For that reason, we have analyzed switching and biofilm formation in *MTL*-homozygous strains of *C. dubliniensis* by comparing them with *C. albicans*. A summary of the results of this comparison is presented in Table 3.

The white-opaque transition. The capacity for *MTL*-homozygous white cells of *C. albicans* and *C. dubliniensis* to switch from white to opaque has been shown to be basic to mating (16, 28, 29) and, in the case of *C. albicans*, to the formation of a white cell

TABLE 3 Comparison between *C. albicans* and *C. dubliniensis* developmental traits and responses of *MTL*-homozygous cells analyzed in this study[a]

Developmental program or response	Aspect	% of strains or means ± SD of traits (no. of strains tested)	
		C. albicans	*C. dubliniensis*
Switching	Wh-to-Op switching among strains[b]	85% (26)	56% (27)
	Op stability among strains[b,c]	94% (22)	27% (15)
	Wh-to-Op switching frequency[d]	1.4×10^{-3} (5)	$<3 \times 10^{-4}$ (5)
	Op-to-Wh switching frequency (Op stability)[d]	1.4×10^{-1} (5)	5.0×10^{-1} (5)
	Alt colony formation by Op cells[d]	0% (5)	100% (5)
	Wh-to-Op switching in CO_2	9×10^{-1} (5)	1.2×10^{-3} (5)
	Op-to-Wh switching in CO_2 (Op stability)	$<6 \times 10^{-3}$ (5)	1×10^{-1} (5)
Cell phenotypes	Uniformity of Wh cell phenotype within each strain	100% (5)	100% (5)
	Uniformity of Op cell phenotype within each strain	100% (5)	0% (5)
Stimulation of planktonic white cells by pheromone or minority Op cells	Adhesion to plastic	100% (10)	100% (15)
Biofilm formation	Basal yeast cell polylayer	100% (12)	100% (8)
	Homogeneous basal yeast cell polylayer	100% (12)	62% (8)
	Upper layer of vertical hyphae	100% (12)	0% (8)
	Upper layer of pseudohyphae	0% (12)	87% (8)
	Dense ECM in upper layer	100% (12)	0% (8)
	Biofilm thickness (unstimulated)[e]	57 ± 3 μm (12)	37 ± 5 μm (8)
	Biofilm thickness (stimulated)[e]	72 ± 5 μm (5)	51 ± 4 μm (3)
	Biofilm dry wt (unstimulated)[e]	0.75 ± 0.13 mg (10)	0.67 ± 0.29 mg (15)
	Biofilm dry wt (stimulated)[e]	0.88 ± 0.12 mg (10)	0.89 ± 0.21 mg (15)
	Op cell stimulation of thickness	100% (5)	100% (3)
	Op cell stimulation of dry wt	90% (10)	87% (15)

[a] Op, opaque; Wh, white; wt, weight.
[b] Data from serial high-density plating experiments (~300 colonies per plate).
[c] Strains in which <10% of the opaque cells plated formed white colonies.
[d] Data from serial low-density plating experiments (~30 to 50 colonies per plate).
[e] Unstimulated, without addition of 10% opaque cells (**a**/**a** + α/α); stimulated, with addition of 10% opaque cells.

biofilm (32). Previously, using a lower threshold for switching, we showed that one-half of 27 *MTL*-homozygous *C. dubliniensis* strains switched (16), but we did not compare variability side by side with a set of randomly selected *C. albicans* strains. Nor did we compare the frequencies of individual strains. Here, using high-density serial plating of white cells, resulting in approximately 15,000 total colonies, we found that the proportion of strains that formed one or more opaque colonies or sectors was 85% of 26 natural *C. albicans* strains and 56% of 27 natural *C. dubliniensis* strains. Then, in a comparison of five random *C. albicans* strains that switched from white to opaque, using low-density plating and five *C. dubliniensis* strains that exhibited the highest switching frequencies in the initial high-density plating experiments, we used low-density plating to assess frequency. We found that the average switching frequency from white to opaque was far higher in random *C. albicans* strains, as was the stability of the opaque phenotype. Phenotypic instability of the opaque phenotype was accompanied by a high level of variability of cellular phenotypes in the opaque cell population of each *MTL*-homozygous strain of *C. dubliniensis*. We further found that a high concentration of CO_2, which causes mass conversion of white to opaque and nearly complete stabilization of the opaque phenotype in *C. albicans* (50), had no effect on *C. dubliniensis*. High CO_2 neither induced switching nor stabilized the opaque phenotype. The possible ramifications of these differences are profound. First, the decrease in switching frequencies from white to opaque and the instability of the opaque phenotype in *C. dubliniensis* strains would affect the efficiency of mating, especially in natural niches such as the gastrointestinal tract and tissues of the host, which maintain high CO_2 levels (62, 63). Second, the decrease in the frequency of white-to-opaque switching and the increase in opaque instability would negatively impact the capacity of *MTL*-homozygous *C. dubliniensis* white cells to form complex biofilms, which has been shown in *C. albicans* to facilitate mating between minority opaque cells that appear through spontaneous switching (32). It would suggest that the mating event would be even rarer among *C. dubliniensis* than among *C. albicans* strains.

Pheromone response and biofilm formation. The experimental model that we have used to form complex biofilms of *MTL*-heterozygous and *MTL*-homozygous cells (31, 34–36) was derived from that of Douglas and coworkers in the 1990s (51–53). Because it had been shown that in the formation of biofilms by *MTL*-homozygous white cells of *C. albicans*, pheromone stimulates adhesion, the first step in *MTL*-homozygous biofilm formation (32, 33, 37), we tested pheromone-stimulated adhesion in white cells of 15 strains of *C. dubliniensis*. The induction of adhesion was approximately 100-fold for all of the 10 test strains of *C. albicans* and all of the 15 test strains of *C. dubliniensis*. The variability between strains was similar, demonstrating the conservation of this trait. In addition, the morphologies of planktonic white-phase cells of five *MTL*-homozygous test strains of *C. albicans* and of five strains of *C. dubliniensis* were found similarly

round and relatively uniform in size. Hence, *MTL*-homozygous strains of *C. dubliniensis* and *C. albicans* have similarly conserved both the yeast phase morphology of white cells and their initial responses to pheromone.

However, the architecture of both the mature *MTL*-heterozygous and *MTL*-homozygous biofilms formed by *C. dubliniensis* not only differed from that of *C. albicans* but also exhibited much higher architectural variability. In biofilms formed by the three tested *C. albicans* **a**/α strains, cells formed a basal yeast cell polylayer and an upper layer of vertically oriented hyphae encapsulated in ECM, as has previously been described (34, 35). The uniformity of the architecture among the three *C. albicans* **a**/α strains was high. Of the six **a**/α *C. dubliniensis* strains, four formed a basal yeast cell polylayer but two did not. Of the four that did, three formed upper regions composed primarily of pseudohyphae. The two without basal yeast cell polylayers formed biofilms composed predominately of pseudohyphae. One strain, B71507, formed a basal yeast cell polylayer and an upper region of both pseudohyphae and patches of vertically oriented hyphae encapsulated in ECM, the latter very similar in architecture to the biofilms of **a**/α *C. albicans*. The propensity for pseudohyphae rather than true hyphae in *C. dubliniensis* **a**/α biofilm was first reported 14 years ago for strain NCPF3949 by Ramage et al. (22), but the *MTL* configuration of that strain was unknown.

For the 12 *MTL*-homozygous *C. albicans* strains, the biofilms formed by white cell populations in the absence of added minority opaque cells were again architecturally uniform, including a basal yeast cell polylayer and an upper region of vertically oriented hyphae encapsulated in ECM. For all eight *MTL*-homozygous *C. dubliniensis* strains, the biofilms formed by white cells in the absence of added minority opaque cells were not architecturally uniform. All contained basal yeast cell polylayers, but the basal layers varied in thickness, and in three strains, there was a minority of pseudohyphae and hyphae. Seven of the eight strains formed pseudohyphal upper regions of variable thickness, but none formed a uniform upper region or even patches of vertically oriented hyphae. One strain, d81217 (**a**/**a**), formed no pseudohyphae or hyphae.

Biofilm thickness and dry weight. Both *MTL*-heterozygous and *MTL*-homozygous biofilms of *C. albicans* formed by white cells in the absence of added opaque cells were thicker than those of *C. dubliniensis*. Of all of the *C. dubliniensis* biofilms analyzed, including **a**/α, **a/a,** and α/α, the thickest was that of the **a**/α strain B71507, which was the only strain that contained vertical hyphae in the upper region. But it was still 23% thinner than the average **a**/α *C. albicans* biofilm. B71507 also contained the most intensely staining ECM. Even though the average thickness of *MTL*-homozygous *C. dubliniensis* biofilms was significantly less than that of *MTL*-homozygous *C. albicans* biofilms, the average dry weight was similar. This inconsistency appears to reflect a difference in cellular density. We have shown here that the cellular compartments of pseudohyphae contain more particulate cytoplasm than do true hyphae, which are highly vacuolated and hence must contain more water. In addition, the mesh of pseudohyphae in *C. dubliniensis* biofilms appeared more compact than the array of vertical hyphae in *C. albicans*, and the pseudohyphae were thicker than the vertically oriented, true hyphae. Finally, the increased ECM of *C. albicans* biofilms may also contribute to a decrease in density, given that the ECM may be a gel made up predominately of water. The similarity of dry weights between the two species suggests that a mechanism that regulates mass has been conserved in both species and that final mass is independent of cellular phenotype and ECM deposition.

Opaque cell stimulation of biofilms. It has been demonstrated that the addition of minority opaque cells, a source of pheromone, to white cells, stimulates final biofilm thickness (32–34, 36, 54). Here, we have shown that minority opaque cells, either of *C. dubliniensis* or *C. albicans*, stimulate the thickness of *MTL*-homozygous white cell biofilms of *C. dubliniensis*. Minority opaque cells of *C. albicans* are more effective than those of *C. dubliniensis*, presumably because the opaque phenotype of *C. dubliniensis* is extremely unstable (16; data shown here). More importantly, the thickness of the biofilms of all five tested *C. albicans* strains and all three tested *C. dubliniensis* strains was stimulated. Using only minority opaque cells of *C. albicans*, we also found that 90% of the dry weight of the biofilms formed by 10 *C. albicans* strains and 87% of 15 *C. dubliniensis* strains were stimulated. Together, these results indicate that opaque cell stimulation of biofilms is similarly conserved in both *C. albicans* and *C. dubliniensis*.

Evolution of a pseudohypha-dominated biofilm. We have found that while several developmental traits of *MTL*-homozygous white cells of *C. dubliniensis*, compared with *MTL* white cells of *C. albicans*, appear to either be degenerating or have been lost, other traits have been conserved. Most importantly, the traits that have been conserved are related to *MTL*-homozygous biofilm development. In this context, the predominance of pseudohyphae could have two alternative explanations. First, it could be considered the degeneration of a program that originally evolved to generate a hypha-dominated biofilm, which has remained intact in *C. albicans*. It is reasonable to suggest that this is the case for two reasons. First, *C. tropicalis* appears to form biofilms dominated by true hyphae (64). It diverged from the ancestor of *C. albicans* and *C. dubliniensis* approximately 30 million years ago, before the separation of the latter species (12). Therefore, a hypha-dominated biofilm may be considered to have preceded the pseudohypha-dominated biofilm formed by *C. dubliniensis*. Second, of all of the **a**/α, α/α, and **a**/**a** *C. dubliniensis* strains tested, strain B71507 formed a biofilm containing subregions of vertically oriented hyphae and increased ECM, architectural traits of the upper region of *C. albicans* biofilms. This suggests that this trait of B71507 biofilms is vestigial. However, if the loss of a hypha-dominated biofilm represents a degenerative process in *C. dubliniensis*, why would other biofilm-related traits, including the cellular phenotype of white cells, pheromone-stimulated adhesion of white cells, opaque cell stimulation of biofilm thickness, biofilm dry weight, and opaque cell stimulation of dry weight, all be conserved in *C. dubliniensis*? An alternative explanation is that *C. dubliniensis* is transitioning from a hypha- to a pseudohypha-dominated biofilm due to different selective pressures. Two aspects of *C. dubliniensis* colonization may provide insight into those selective pressures. First, *C. dubliniensis* is more often recovered from oropharyngeal samples (11). Second, *C. dubliniensis* is isolated in a majority of cases in combination with *C. albicans* (65–68), which could explain why opaque cells of *C. albicans* are more stimulatory than opaque cells of *C. dubliniensis* in the growth of a *C. dubliniensis* biofilm. This evolutionary puzzle, therefore, warrants further exploration.

ACKNOWLEDGMENTS

We are indebted to Sandra Beck for help in assembling the manuscript, and we acknowledge the technical support and expertise provided by Randy Nessler and the CMRF at UI.

This project was supported by the Developmental Studies Hybridoma Bank, a National Resource created by the NIH and housed at the University of Iowa.

REFERENCES

1. **Fong DW, Kane TC, Culver DC.** 1995. Vestigialization and loss of nonfunctional characters. Annu Rev Ecol Syst **26:**249–268. http://dx.doi.org/10.1146/annurev.es.26.110195.001341.
2. **Lahti DC, Johnson NA, Ajie BC, Otto SP, Hendry AP, Blumstein DT, Coss RG, Donohue K, Foster SA.** 2009. Relaxed selection in the wild. Trends Ecol Evol **24:**487–496. http://dx.doi.org/10.1016/j.tree.2009.03.010.
3. **Porter M, Crandall KA.** 2003. Lost along the way: the significance of evolution in reverse. Trends Ecol Evol **18:**541–547. http://dx.doi.org/10.1016/S0169-5347(03)00244-1.
4. **Hall AR, Colegrave N.** 2007. How does resource supply affect evolutionary diversification? Proc Biol Sci **274:**73–78. http://dx.doi.org/10.1098/rspb.2006.3703.
5. **Hall AR, Colegrave N.** 2008. Decay of unused characters by selection and drift. J Evol Biol **21:**610–617. http://dx.doi.org/10.1111/j.1420-9101.2007.01473.x.
6. **Kimura M.** 1983. The neutral theory of molecular evolution. Cambridge University Press, Cambridge, United Kingdom.
7. **Maughan H, Masel J, Birky CW, Jr, Nicholson WL.** 2007. The roles of mutation accumulation and selection in loss of sporulation in experimental populations of Bacillus subtilis. Genetics **177:**937–948. http://dx.doi.org/10.1534/genetics.107.075663.
8. **McManus BA, Coleman DC.** 2014. Molecular epidemiology, phylogeny and evolution of Candida albicans. Infect Genet Evol **21:**166–178. http://dx.doi.org/10.1016/j.meegid.2013.11.008.
9. **Moran GP, Coleman DC, Sullivan DJ.** 2012. Candida albicans versus Candida dubliniensis: why is C. albicans more pathogenic? Int J Microbiol **2012:**205921. http://dx.doi.org/10.1155/2012/205921.
10. **Sullivan D, Coleman D.** 1997. Candida dubliniensis: an emerging opportunistic pathogen. Curr Top Med Mycol **8:**15–25.
11. **Sullivan DJ, Moran GP, Coleman DC.** 2005. Candida dubliniensis: ten years on. FEMS Microbiol Lett **253:**9–17. http://dx.doi.org/10.1016/j.femsle.2005.09.015.
12. **Mishra NN, Prasad T, Sharma N, Payasi A, Prasad R, Gupta DK, Singh R.** 2007. Pathogenicity and drug resistance in Candida albicans and other yeast species. A review. Acta Microbiol Immunol Hung **54:**201–235. http://dx.doi.org/10.1556/AMicr.54.2007.3.1.
13. **Jackson AP, Gamble JA, Yeomans T, Moran GP, Saunders D, Harris D, Aslett M, Barrell JF, Butler G, Citiulo F, Coleman DC, de Groot PW, Goodwin TJ, Quail MA, McQuillan J, Munro CA, Pain A, Poulter RT, Rajandream MA, Renauld H, Spiering MJ, Tivey A, Gow NA, Barrell B, Sullivan DJ, Berriman M.** 2009. Comparative genomics of the fungal pathogens Candida dubliniensis and Candida albicans. Genome Res **19:**2231–2244. http://dx.doi.org/10.1101/gr.097501.109.
14. **Sheth CC, Johnson E, Baker ME, Haynes K, Muhlschlegel FA.** 2005. Phenotypic identification of Candida albicans by growth on chocolate agar. Med Mycol **43:**735–738. http://dx.doi.org/10.1080/13693780500265998.
15. **Stokes C, Moran GP, Spiering MJ, Cole GT, Coleman DC, Sullivan DJ.** 2007. Lower filamentation rates of Candida dubliniensis contribute to its lower virulence in comparison with Candida albicans. Fungal Genet Biol **44:**920–931. http://dx.doi.org/10.1016/j.fgb.2006.11.014.
16. **Pujol C, Daniels KJ, Lockhart SR, Srikantha T, Radke JB, Geiger J, Soll DR.** 2004. The closely related species Candida albicans and Candida dubliniensis can mate. Eukaryot Cell **3:**1015–1027. http://dx.doi.org/10.1128/EC.3.4.1015-1027.2004.
17. **Hannula J, Saarela M, Alaluusua S, Slots J, Asikainen S.** 1997. Phenotypic and genotypic characterization of oral yeasts from Finland and the United States. Oral Microbiol Immunol **12:**358–365. http://dx.doi.org/10.1111/j.1399-302X.1997.tb00739.x.
18. **Sullivan DJ, Moran GP, Pinjon E, Al-Mosaid A, Stokes C, Vaughan C, Coleman DC.** 2004. Comparison of the epidemiology, drug resistance mechanisms, and virulence of Candida dubliniensis and Candida albicans. FEMS Yeast Res **4:**369–376. http://dx.doi.org/10.1016/S1567-1356(03)00240-X.
19. **Vilela MM, Kamei K, Sano A, Tanaka R, Uno J, Takahashi I, Ito J, Yarita K, Miyaji M.** 2002. Pathogenicity and virulence of Candida dubliniensis: comparison with C. albicans. Med Mycol **40:**249–257.
20. **Gilfillan GD, Sullivan DJ, Haynes K, Parkinson T, Coleman DC, Gow NA.** 1998. Candida dubliniensis: phylogeny and putative virulence factors. Microbiology **144**(Part 4)**:**829–838. http://dx.doi.org/10.1099/00221287-144-4-829.
21. **Staib P, Morschhauser J.** 1999. Chlamydospore formation on Staib agar as a species-specific characteristic of Candida dubliniensis. Mycoses **42:**521–524. http://dx.doi.org/10.1046/j.1439-0507.1999.00516.x.
22. **Ramage G, Vande Walle K, Wickes BL, Lopez-Ribot JL.** 2001. Biofilm formation by Candida dubliniensis. J Clin Microbiol **39:**3234–3240. http://dx.doi.org/10.1128/JCM.39.9.3234-3240.2001.
23. **Moran GP, Coleman DC, Sullivan DJ.** 2011. Comparative genomics and the evolution of pathogenicity in human pathogenic fungi. Eukaryot Cell **10:**34–42. http://dx.doi.org/10.1128/EC.00242-10.
24. **Joly S, Pujol C, Rysz M, Vargas K, Soll DR.** 1999. Development and characterization of complex DNA fingerprinting probes for the infectious yeast Candida dubliniensis. J Clin Microbiol **37:**1035–1044.
25. **Joly S, Pujol C, Soll DR.** 2002. Microevolutionary changes and chromosomal translocations are more frequent at RPS loci in Candida dubliniensis than in Candida albicans. Infect Genet Evol **2:**19–37. http://dx.doi.org/10.1016/S1567-1348(02)00058-8.
26. **Magee BB, Sanchez MD, Saunders D, Harris D, Berriman M, Magee PT.** 2008. Extensive chromosome rearrangements distinguish the karyotype of the hypovirulent species Candida dubliniensis from the virulent Candida albicans. Fungal Genet Biol **45:**338–350. http://dx.doi.org/10.1016/j.fgb.2007.07.004.
27. **Odds FC, Bougnoux ME, Shaw DJ, Bain JM, Davidson AD, Diogo D, Jacobsen MD, Lecomte M, Li SY, Tavanti A, Maiden MC, Gow NA, d'Enfert C.** 2007. Molecular phylogenetics of Candida albicans. Eukaryot Cell **6:**1041–1052. http://dx.doi.org/10.1128/EC.00041-07.
28. **Lockhart SR, Pujol C, Daniels KJ, Miller MG, Johnson AD, Pfaller MA, Soll DR.** 2002. In Candida albicans, white-opaque switchers are homozygous for mating type. Genetics **162:**737–745.
29. **Miller MG, Johnson AD.** 2002. White-opaque switching in Candida albicans is controlled by mating-type locus homeodomain proteins and allows efficient mating. Cell **110:**293–302. http://dx.doi.org/10.1016/S0092-8674(02)00837-1.
30. **Lockhart SR, Zhao R, Daniels KJ, Soll DR.** 2003. Alpha-pheromone-induced "shmooing" and gene regulation require white-opaque switching during Candida albicans mating. Eukaryot Cell **2:**847–855. http://dx.doi.org/10.1128/EC.2.5.847-855.2003.
31. **Park YN, Daniels KJ, Pujol C, Srikantha T, Soll DR.** 2013. Candida albicans forms a specialized "sexual" as well as "pathogenic" biofilm. Eukaryot Cell **12:**1120–1131. http://dx.doi.org/10.1128/EC.00112-13.
32. **Yi S, Sahni N, Daniels KJ, Lu KL, Srikantha T, Huang G, Garnaas AM, Soll DR.** 2011. Alternative mating type configurations (a/alpha versus a/a or alpha/alpha) of Candida albicans result in alternative biofilms regulated by different pathways. PLoS Biol **9:**e1001117. http://dx.doi.org/10.1371/journal.pbio.1001117.
33. **Yi S, Sahni N, Daniels KJ, Pujol C, Srikantha T, Soll DR.** 2008. The same receptor, G protein, and mitogen-activated protein kinase pathway activate different downstream regulators in the alternative white and opaque pheromone responses of Candida albicans. Mol Biol Cell **19:**957–970.
34. **Daniels KJ, Srikantha T, Pujol C, Park YN, Soll DR.** 2015. Role of Tec1 in the development, architecture, and integrity of sexual biofilms of Candida albicans. Eukaryot Cell **14:**228–240. http://dx.doi.org/10.1128/EC.00224-14.
35. **Daniels KJ, Park YN, Srikantha T, Pujol C, Soll DR.** 2013. The impact of environmental conditions on the form and function of Candida albicans biofilms. Eukaryot Cell **12:**1389–1402. http://dx.doi.org/10.1128/EC.00127-13.
36. **Daniels KJ, Srikantha T, Lockhart SR, Pujol C, Soll DR.** 2006. Opaque cells signal white cells to form biofilms in Candida albicans. EMBO J **25:**2240–2252. http://dx.doi.org/10.1038/sj.emboj.7601099.
37. **Lin CH, Kabrawala S, Fox EP, Nobile CJ, Johnson AD, Bennett RJ.** 2013. Genetic control of conventional and pheromone-stimulated biofilm formation in Candida albicans. PLoS Pathog **9:**e1003305. http://dx.doi.org/10.1371/journal.ppat.1003305.
38. **Wu W, Lockhart SR, Pujol C, Srikantha T, Soll DR.** 2007. Heterozy-

gosity of genes on the sex chromosome regulates Candida albicans virulence. Mol Microbiol **64:**1587–1604. http://dx.doi.org/10.1111/j.1365-2958.2007.05759.x.
39. **Bedell GW, Soll DR.** 1979. Effects of low concentrations of zinc on the growth and dimorphism of Candida albicans: evidence for zinc-resistant and -sensitive pathways for mycelium formation. Infect Immun **26:**348–354.
40. **Lee KL, Buckley HR, Campbell CC.** 1975. An amino acid liquid synthetic medium for the development of mycelial and yeast forms of Candida albicans. Sabouraudia **13:**148–153. http://dx.doi.org/10.1080/00362177585190271.
41. **Anderson JM, Soll DR.** 1987. Unique phenotype of opaque cells in the white-opaque transition of Candida albicans. J Bacteriol **169:**5579–5588.
42. **McCullough MJ, Clemons KV, Stevens DA.** 1999. Molecular and phenotypic characterization of genotypic Candida albicans subgroups and comparison with Candida dubliniensis and Candida stellatoidea. J Clin Microbiol **37:**417–421.
43. **Romeo O, Criseo G.** 2008. First molecular method for discriminating between Candida africana, Candida albicans, and Candida dubliniensis by using hwp1 gene. Diagn Microbiol Infect Dis **62:**230–233. http://dx.doi.org/10.1016/j.diagmicrobio.2008.05.014.
44. **Sahni N, Yi S, Daniels KJ, Srikantha T, Pujol C, Soll DR.** 2009. Genes selectively up-regulated by pheromone in white cells are involved in biofilm formation in Candida albicans. PLoS Pathog **5:**e1000601. http://dx.doi.org/10.1371/journal.ppat.1000601.
45. **Slutsky B, Staebell M, Anderson J, Risen L, Pfaller M, Soll DR.** 1987. "White-opaque transition": a second high-frequency switching system in Candida albicans. J Bacteriol **169:**189–197.
46. **Porman AM, Alby K, Hirakawa MP, Bennett RJ.** 2011. Discovery of a phenotypic switch regulating sexual mating in the opportunistic fungal pathogen Candida tropicalis. Proc Natl Acad Sci U S A **108:**21158–21163. http://dx.doi.org/10.1073/pnas.1112076109.
47. **Huang G, Wang H, Chou S, Nie X, Chen J, Liu H.** 2006. Bistable expression of WOR1, a master regulator of white-opaque switching in Candida albicans. Proc Natl Acad Sci U S A **103:**12813–12818. http://dx.doi.org/10.1073/pnas.0605270103.
48. **Srikantha T, Borneman AR, Daniels KJ, Pujol C, Wu W, Seringhaus MR, Gerstein M, Yi S, Snyder M, Soll DR.** 2006. TOS9 regulates white-opaque switching in Candida albicans. Eukaryot Cell **5:**1674–1687. http://dx.doi.org/10.1128/EC.00252-06.
49. **Zordan RE, Galgoczy DJ, Johnson AD.** 2006. Epigenetic properties of white-opaque switching in Candida albicans are based on a self-sustaining transcriptional feedback loop. Proc Natl Acad Sci U S A **103:**12807–12812. http://dx.doi.org/10.1073/pnas.0605138103.
50. **Huang G, Srikantha T, Sahni N, Yi S, Soll DR.** 2009. CO(2) regulates white-to-opaque switching in Candida albicans. Curr Biol **19:**330–334. http://dx.doi.org/10.1016/j.cub.2009.01.018.
51. **Hawser SP, Baillie GS, Douglas LJ.** 1998. Production of extracellular matrix by Candida albicans biofilms. J Med Microbiol **47:**253–256. http://dx.doi.org/10.1099/00222615-47-3-253.
52. **Hawser SP, Douglas LJ.** 1994. Biofilm formation by Candida species on the surface of catheter materials in vitro. Infect Immun **62:**915–921.
53. **Hawser SP, Douglas LJ.** 1995. Resistance of Candida albicans biofilms to antifungal agents in vitro. Antimicrob Agents Chemother **39:**2128–2131. http://dx.doi.org/10.1128/AAC.39.9.2128.
54. **Yi S, Sahni N, Pujol C, Daniels KJ, Srikantha T, Ma N, Soll DR.** 2009. A Candida albicans-specific region of the alpha-pheromone receptor plays a selective role in the white cell pheromone response. Mol Microbiol **71:**925–947. http://dx.doi.org/10.1111/j.1365-2958.2008.06575.x.
55. **Wolf YI, Koonin EV.** 2013. Genome reduction as the dominant mode of evolution. Bioessays **35:**829–837. http://dx.doi.org/10.1002/bies.201300037.
56. **Pfaller MA, Diekema DJ.** 2007. Epidemiology of invasive candidiasis: a persistent public health problem. Clin Microbiol Rev **20:**133–163. http://dx.doi.org/10.1128/CMR.00029-06.
57. **Kibbler CC, Seaton S, Barnes RA, Gransden WR, Holliman RE, Johnson EM, Perry JD, Sullivan DJ, Wilson JA.** 2003. Management and outcome of bloodstream infections due to Candida species in England and Wales. J Hosp Infect **54:**18–24. http://dx.doi.org/10.1016/S0195-6701(03)00085-9.
58. **Moran GP, MacCallum DM, Spiering MJ, Coleman DC, Sullivan DJ.** 2007. Differential regulation of the transcriptional repressor NRG1 accounts for altered host-cell interactions in Candida albicans and Candida dubliniensis. Mol Microbiol **66:**915–929. http://dx.doi.org/10.1111/j.1365-2958.2007.05965.x.
59. **Tavanti A, Davidson AD, Fordyce MJ, Gow NA, Maiden MC, Odds FC.** 2005. Population structure and properties of Candida albicans, as determined by multilocus sequence typing. J Clin Microbiol **43:**5601–5613. http://dx.doi.org/10.1128/JCM.43.11.5601-5613.2005.
60. **Srikantha T, Daniels KJ, Pujol C, Kim E, Soll DR.** 2013. Identification of genes upregulated by the transcription factor Bcr1 that are involved in impermeability, impenetrability and drug-resistance of Candida albicans a/alpha biofilms. Eukaryot Cell **12:**875–888. http://dx.doi.org/10.1128/EC.00071-13.
61. **Srikantha T, Daniels KJ, Pujol C, Sahni N, Yi S, Soll DR.** 2012. Nonsex genes in the mating type locus of Candida albicans play roles in a/alpha biofilm formation, including impermeability and fluconazole resistance. PLoS Pathog **8:**e1002476. http://dx.doi.org/10.1371/journal.ppat.1002476.
62. **Aunduk C.** 2002. Manual of gastroenterology: diagnosis and therapy. Lippincott, Williams & Wilkins, Philadelphia, PA.
63. **Levitt MD, Bond JH, Jr.** 1970. Volume, composition, and source of intestinal gas. Gastroenterology **59:**921–929.
64. **Marcos-Zambrano LJ, Escribano P, Bouza E, Guinea J.** 2014. Production of biofilm by Candida and non-Candida spp. isolates causing fungemia: comparison of biomass production and metabolic activity and development of cut-off points. Int J Med Microbiol **304:**1192–1198. http://dx.doi.org/10.1016/j.ijmm.2014.08.012.
65. **Ho MW, Yang YL, Lin CC, Chi CY, Chen HT, Lin PC, Hsieh LY, Chou CH, Chu WL, Wu CP, Lauderdale TL, Lo HJ.** 2014. Yeast oropharyngeal colonization in human immunodeficiency virus-infected patients in central Taiwan. Mycopathologia **177:**309–317. http://dx.doi.org/10.1007/s11046-014-9753-5.
66. **Ieda S, Moriyama M, Takeshita T, Maehara T, Imabayashi Y, Shinozaki S, Tanaka A, Hayashida JN, Furukawa S, Ohta M, Yamashita Y, Nakamura S.** 2014. Molecular analysis of fungal populations in patients with oral candidiasis using internal transcribed spacer region. PLoS One **9:**e101156. http://dx.doi.org/10.1371/journal.pone.0101156.
67. **Masoud-Landgraf L, Badura A, Eber E, Feierl G, Marth E, Buzina W.** 2014. Modified culture method detects a high diversity of fungal species in cystic fibrosis patients. Med Mycol **52:**179–186.
68. **McManus BA, Maguire R, Cashin PJ, Claffey N, Flint S, Abdulrahim MH, Coleman DC.** 2012. Enrichment of multilocus sequence typing clade 1 with oral Candida albicans isolates in patients with untreated periodontitis. J Clin Microbiol **50:**3335–3344. http://dx.doi.org/10.1128/JCM.01532-12.